A STUDY OF DROPWISE CONDENSATION

Thesis for the Degree of Ph. D.

MICHIGAN STATE UNIVERSITY

Ronald Luther Reisbig

1966

THESIS

LIBRARY
Michigan State
University

This is to certify that the

thesis entitled

A Study of Dropwise Condensation

presented by

Ronald Luther Reisbig

has been accepted towards fulfillment
of the requirements for

Ph.D. degree in Mechanical Engineering

J. E. Lay
Major professor

Date August 9, 1966

O-169

MAR 2 9 2007
C71001

ABSTRACT

A STUDY OF DROPWISE CONDENSATION

by Ronald L. Reisbig

Dropwise condensation of water vapor was studied on a verticle 1 foot high copper surface having an area of 1 ft.^{2}. Dropwise condensation was promoted by coating the surface with a 0.0017 inch thick film of polytetrafluoroethylene (teflon). Two experiments were performed to study the phenomenon. A heat transfer experiment was made to determine the heat flux and the heat transfer coefficient as a function of condenser surface temperature. The mechanism of dropwise condensation was studied experimentally by taking a series of high speed motion pictures. The pictures were taken at high magnification by using a microscope, and at low magnification without the microscope. The heat transfer conditions were carefully determined while the pictures were being taken.

Dropwise condensation heat transfer coefficients varied from 26,400 BTU/hrft°F to 6,650 BTU/hrft°F over a (T_{sv}-T_s) range of 0.5°F to 7.4°F. Heat flux values were determined up to 49,300 BTU/hrft^2.

The motion pictures were taken at film speeds in

the range 720 to 2500 pictures per second over a $(T_{sv}-T_s)$ range of 1.0°F to 3.4°F. The magnification in the pictures ranged from 0.124X to 18.5X.

As a result of the photographic experiment as well as theoretical analysis, the following mechanism is proposed for dropwise condensation. Droplets obtain a certain critical radius which is determined by the condenser surface temperature. These drops then nucleate at random and preferred condensation sites located on active bare condenser surface. Random sites (with respect to both time and location) number as many as 10^{10} per in.^{2} per second. Preferred sites are wetted pits in the teflon film as well as nonwetted cavities. The wetted pits number about 10^3 per in.^{2} and the nonwetted pits number about 10^6 per in.^{2}. Most of the latent heat is transferred through nucleation sized drops that grow by capturing vapor molecules. After the first collision of the nucleation sized drops, the new drop field grows primarily by coalescence with other drops. The drops continue to grow in this fashion until they roll off from the surface. Drop coalescence and roll-off clean the surface of condensate and create active area on which nucleation again occurs.

This mechanism was used as the basis for the deri-

vation of equations for the heat flux and the heat transfer coefficient. These equations, which were derived using a kinetic theory approach, are shown to correlate very well with the experimental data.

A STUDY OF DROPWISE CONDENSATION

By

Ronald Luther Reisbig

A THESIS

Submitted to
Michigan State University
in partial fulfillment of the requirements
for the degree of

DOCTOR OF PHILOSOPHY

Department of Mechanical Engineering

1966

ACKNOWLEDGEMENTS

The author wishes to express gratitude to Professor J. Lay for his advice and guidance during this program.

Dr. St. Clair is thanked for finding the needed funds to support portions of the research.

To my wife, Barbara, I wish to express the deepest gratitude for her devotion and understanding. She deserves credit not only for typing and helping proofread this thesis, but also for providing a major portion of our family income during this program.

The National Aeronautics and Space Administration, as well as The Ford Foundation is acknowledged for grants and fellowships which gave me the opportunity to study for a Ph.D.

TABLE OF CONTENTS

TABLE OF CONTENTS (CONT.)

LIST OF FIGURES

LIST OF TABLES

LIST OF APPENDICES

NOMENCLATURE

A	area
A_n	surface area of a drop with n molecules
A_{nc}	surface area of a critical sized drop
D	diameter
$D(n)$	distribution function
E	energy
$f(n)$	distribution function
F_m	inactive fraction of the condenser surface area
g_o	gravitational constant
$\bar{h}$	heat transfer coefficient, BTU/hr/ft^2/°F
h_{fg}	heat of vaporization, BTU/hr/lb$_m$
h^*_{fg}	heat of vaporization per molecule
J	nucleation rate, nucleations/sec./in.^{2}
k	thermal conductivity, Boltzmann's constant
k_l	thermal conductivity of the liquid, BTU/hr/ft/°F
L	heighth of the condenser surface
$L(n)$	distribution function
M	mass
$\dot{M}_v$	mass rate of vapor molecules to a surface
M_d	mass of a drop
$\bar{N}$	number of molecules striking a surface
n	number of molecules

n_c	number of molecules in a critical drop
P	pressure
P_r	internal pressure of a drop of size r
P_{vs}	saturated vapor pressure at the surface temperature T_s
P_{sv}	saturated vapor pressure at the vapor temp. T_{sv}
Q	heat flux, BTU/hr/ft^2
r	radius
r_c	critical drop radius
R	gas constant
T	temperature
T_s	condenser surface temperature
T_{sv}	saturated vapor temperature
t	time
U	overall heat transfer coefficient, BTU/hr/ft^2/°F
v	velocity
v_l	specific volume of liquid
v_v	specific volume of vapor
W	work
α	accomodation coefficient
ϵ	evaporation coefficient
ρ	density
σ	surface tension
σ_{sv}	solid-vapor surface tension

σ_{sl} solid-liquid surface tension

σ_{lv} liquid-vapor surface tension

θ contact angle

1.0 INTRODUCTION

A vapor can condense on a surface in either of three ways: "filmwise", wherein the condensate forms a continuous liquid film on the surface; "dropwise", wherein the condensate forms discrete drops on the surface; and "mixed", wherein filmwise and dropwise condensation occur simultaneously. As a mechanism, mixed condensation is the least important of the above three. All three condensation mechanisms produce surface heat transfer coefficients that are large compared with coefficients produced by forced convection processes. Dropwise condensation produces heat fluxes that are an order of magnitude larger than those associated with filmwise condensation for a given value of surface subcooling $(T_{sv}-T_s)$.

While dropwise condensation is the more desirable mechanism, it is the least exploited. This can be explained by the following facts,

1. Dropwise condensation requires a surface that is not wetted by the condensate. Since most common fluids, such as water, wet clean metal surfaces, a nonwetting agent or promoter must be placed between the condensate and the metalic surface. To date few, if any, practical schemes have been proposed

for promoting dropwise condensation.

2. The mechanics of the mechanism of dropwise condensation has not been understood. This has made it impossible to develop a meaningful mathematical analysis of the process.

This research program was undertaken to study the above stated problems, with major emphasis placed on number two.

The original systematic investigation of dropwise condensation was made in 1930 by Schmidt, Schurig and Sellschopp(30)*. Between 1933 and 1935 Drew, et al(7, 8) extended knowledge about the conditions under which either dropwise or filmwise condensation can occur.

There are two schools of thought on the mechanism of dropwise condensation. In 1936 Jakob(20), suggested that the initial drops are formed by an unstable condensate film which fractures and rolls into drops. In the same year Eucken(28) suggested that the drops nucleate. In 1939, Emmons(29) also developed a theory for dropwise condensation that proposes drop nucleation. In recent studies Baer and McKelvey(21) as well as Welch(10) have supported the film fracture concept of Jakob, while

---

*Numbers in parentheses refer to bibliography.

McCormick and Baer(33) as well as Umur and Griffith(13) have supported the drop nucleation concept of Eucken.

By analyzing the conduction across macroscopic drops Fatica and Katz(9) made an initial attempt to develop a mathematical expression for dropwise condensation heat transfer coefficients. Their equation presents the condensation heat transfer coefficient in terms of the overall heat transfer coefficient, which is a major drawback. Sugawara and Michiyoski(27) later extended Fatica's analysis to include the sweeping cycle as well as the adhering period.

Previous methods used to promote dropwise condensation involved using chemical additives in the vapor or oily materials applied directly to the condenser surface. Examples of such additives are stearic and oleic acid, mercaptans, waxes and oils. The common failing of all these techniques is that replenishment is required, that is, the effectiveness of the promoter diminishes with time. Chemical promoters are also adversely effected by dirt and rust present in the steam. Another disadvantage is that these promoters do not work on all base materials commonly used in condenser design. The variation in promoter performance with time helps explain the past disagreement between different sets of dropwise condensation heat transfer data.

The use of thin plastic films which are coated directly onto a condenser surface presents a promising technique for promoting dropwise condensation. Topper and Baer(2) suggested the use of teflon in a 1955 study in which they demonstrated teflons ability to promote dropwise condensation of such organic vapors as ethyleneglycol, nitrobenzene and aniline. A 1958 study by Baer and McKelvey(21) compared the time-life performance of a surface coated with silicone grease, and one coated with teflon. They report that the silicone grease deteriorated after 4 hours, while the teflon surface was not effected after 7 hours of operation. In a 1963 study by Depew and Reisbig(24), teflon was used as the promoter on a horizontal condenser tube. In that study a teflon coating was shown to provide a practical method for promoting dropwise condensation. That study also produced the first significant heat transfer data for dropwise condensation using teflon as a promoter.

This research program was undertaken to determine;

1. Quantitative data for heat transfer to a vertical flat plate condenser surface without the time dependent variables associated with chemical promoters.
2. To study the mechamism of dropwise condensation, and establish the significant parameters. In accordance with Jakob's(20) original

suggestion, the high speed motion picture camera, and microscope were used in this effort.

3. To study the operational effects on teflon films caused by several thousand hours of operation in a steam environment.

4. To improve existing mechanism theories, and develop a mathematical expression for the heat flux and heat transfer coefficient for dropwise condensation.

2.0 HEAT TRANSFER EXPERIMENT

Dropwise condensation tests of the heat transfer from saturated water vapor to a teflon coated vertical condenser surface were made. The tests evaluated the state of the steam, the temperature of the condenser surface and the rate of steam condensation. The experiment was designed so that the state of the steam could be held constant while the condenser surface temperature was changed. By measuring the temperature difference between the saturated steam and the condenser surface, and using measured heat flux data, it was possible to calculate the condensing heat transfer coefficient as a function of this temperature difference. The method is illustrated by the following equation:

$$\bar{h} = \frac{Q}{(T_{sv} - T_s)} \qquad (2.1)$$

Dropwise condensation was promoted and maintained during the tests by a thin coating of teflon. A complete discussion of the dropwise promotion method is presented in section 6.0.

Detailed descriptions of the experimental apparatus are presented in section 2.1. The experimental procedure used during the heat transfer tests is presented in section 2.2. Figure 2.1 and figure 2.2 are photographs of of the research apparatus. Note that these pictures in-

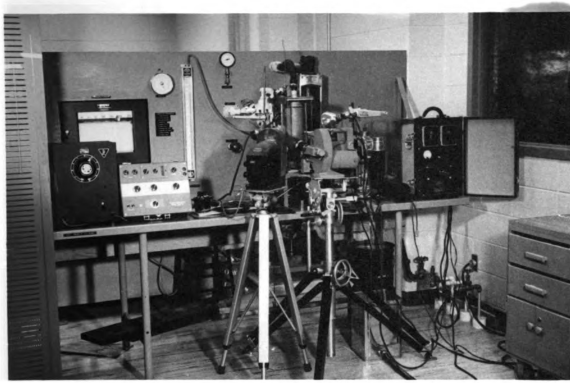

Figure 2.1 The Experimental Apparatus

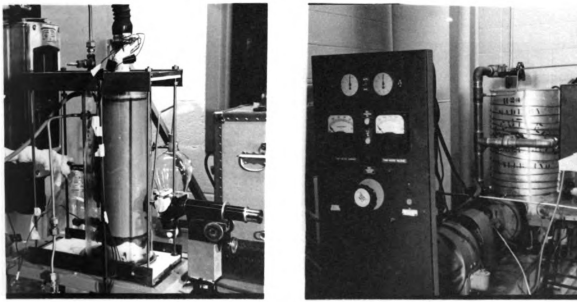

Figure 2.2 The Test Section and Pumping System

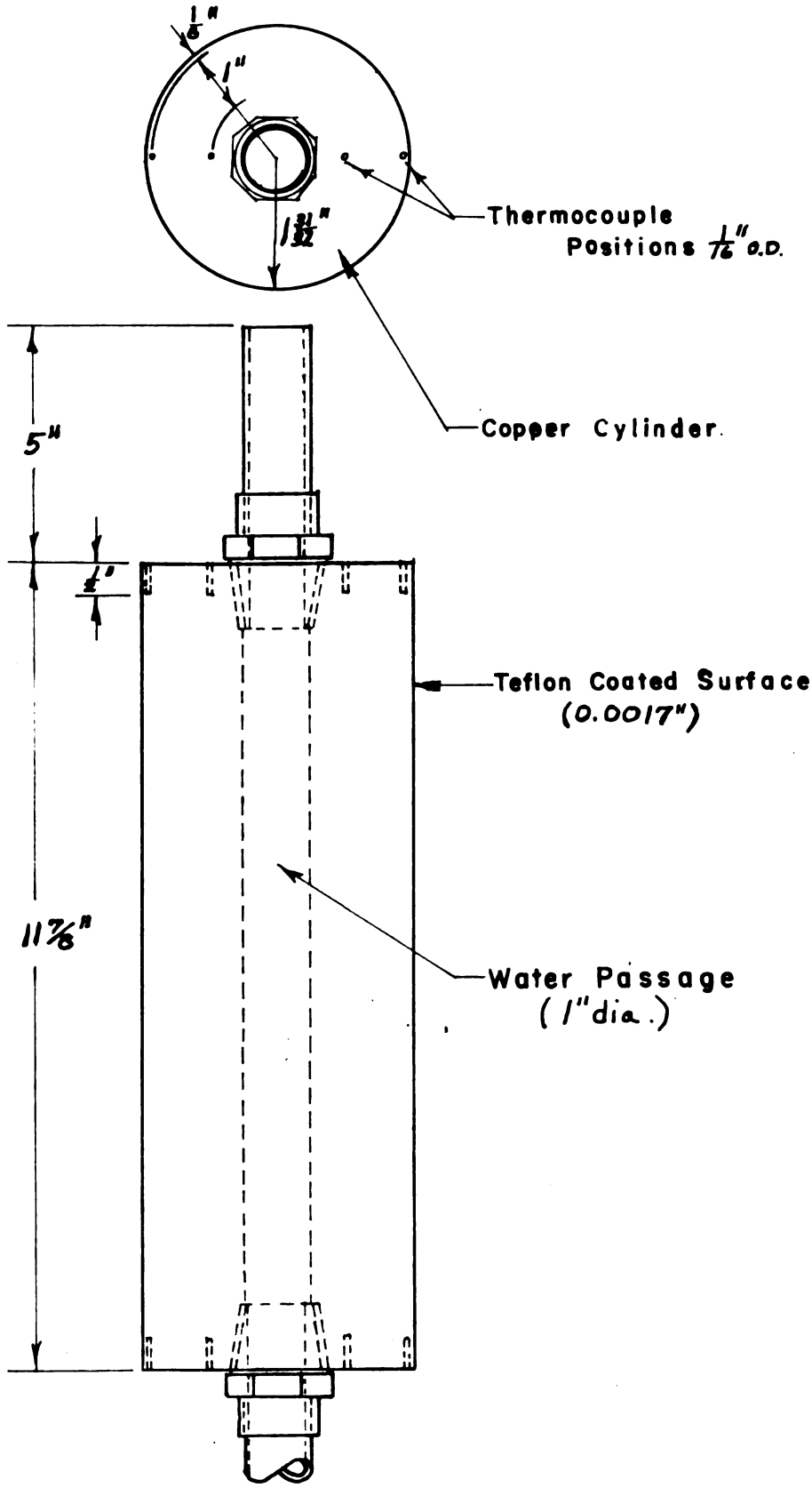

Figure 2.3 Drawing of teflon coated copper condenser surface

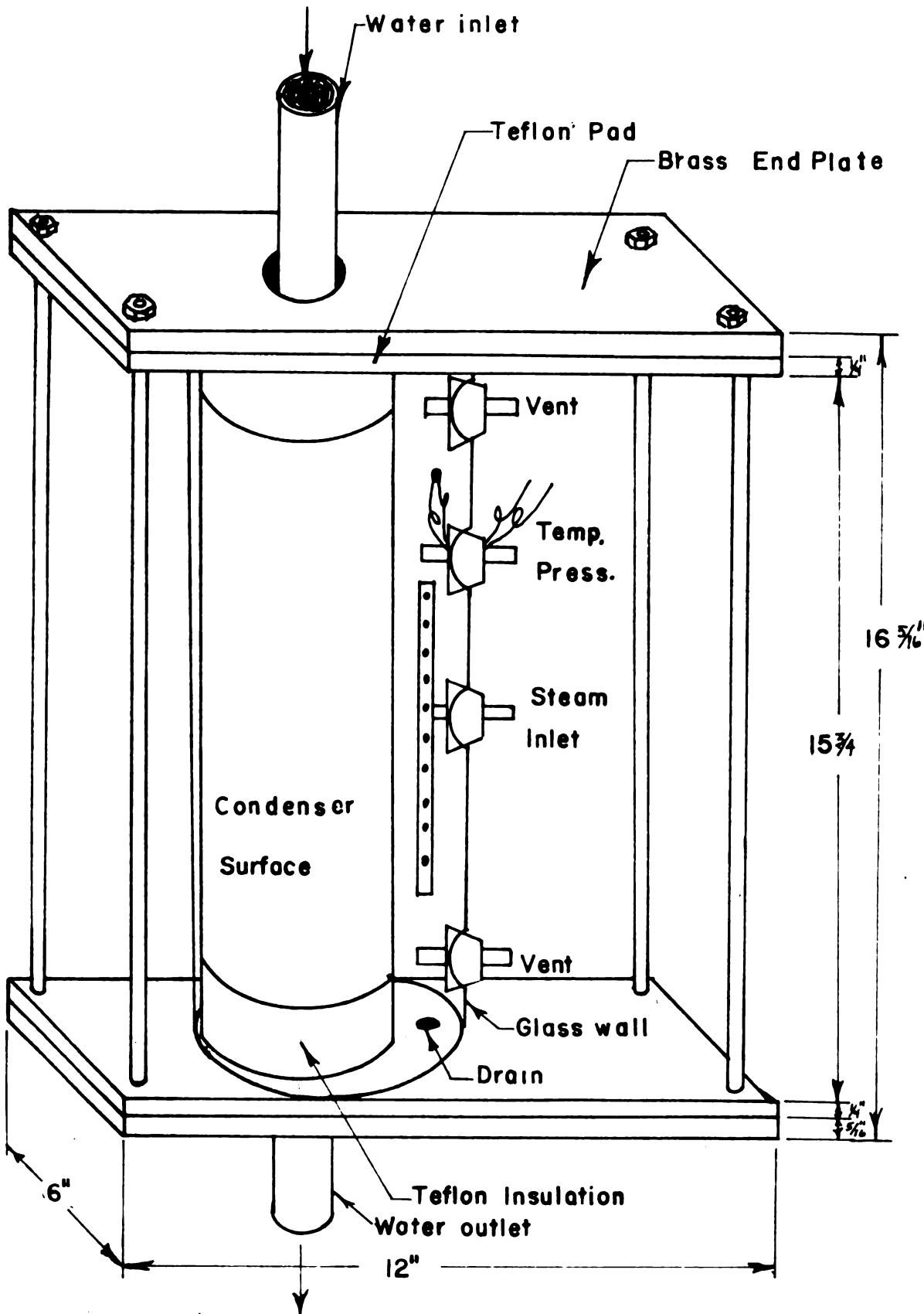

Figure 2.4 Pictorial Drawing of The Test Chamber

clude the photographic and optical equipment as well as the heat transfer apparatus.

2.1 THE EXPERIMENTAL HEAT TRANSFER APPARATUS

The experimental system used in this research was a copper cylinder, 12 inches long and 4 inches outside diameter. The 1 inch inside diameter of the cylinder was used to allow cooling water to pass through the test section. The copper in the cylinder was classed as, "electrolytic tough pitch rod", which is rated by the manufacturer as 99.9 percent pure copper with a maximum of 0.04 percent oxygen. A drawing of the condenser surface is shown in figure 2.3. The 1.5 inch thick copper walls of the test section allowed the condenser surface to be at a uniform temperature regardless of the temperature variation of the cooling water as it passed through the test section. The outside surface of the cylinder was coated with a 0.0017 inch thick film of teflon. Four thermocouples were placed in each end of the copper cylinder. The location of the thermocouples is shown in figure 2.3. The external surfaces of the copper cylinder were machined on a lathe to a grade 32 finish. The outside surface of the copper cylinder wall was polished with Wetordry, Waterproof Silicon Carbide, grit number 320 A, soft-black sandpaper before it was coated with teflon.

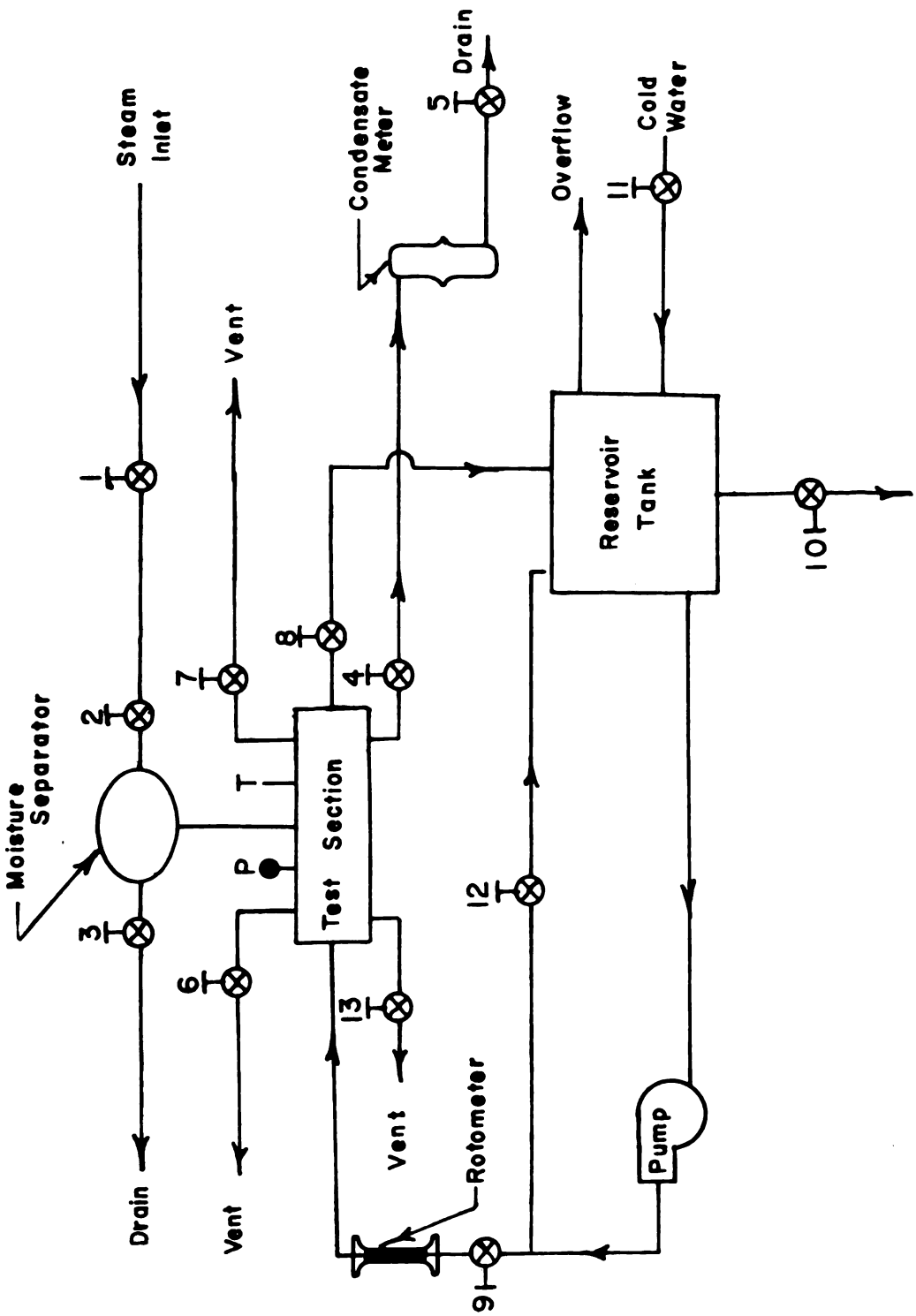

Figure 2.5 Schematic of Experimental Apparatus

A pictorial drawing of the test section assesmbly and steam chamber is shown in figure 2.4. The ends of the copper cylinder were insulated on the bottom by a 2.50 inch long cylinder of teflon and on the top by a 1.25 inch long cylinder of teflon. The outside diameter of these teflon insulation cylinders was the same as the outside diameter of the condenser surface. The end plates of the steam chamber were made of 5/16 inch thick brass, and each was sandwiched with a 0.25 inch pad of teflon. The steam chamber wall was made from a 178mm (5.9 inch) outside diameter section of glass tubing. The walls of the glass tube were 0.15 inches thick and the length of the tube used in the steam chamber was 15.75 inches. Four one inch O.D. holes were made in the glass tube wall to give access to the inside of the steam chamber. Using a glass walled steam chamber allowed a complete observation of the entire condenser surface at all times. Since dropwise condensation is strongly effected by surface contamination, the ability to observe the condition on the condenser surface was most important.

The entire condenser chamber assembly was held together by four ¼ inch brass tie-rods. All steam joints in the chamber were of a mechanical nature requiring force from the tie-rods to implement a good steam tight seal. To insure a steam tight seal of all joints and to correct for the different thermal expansions of the

different materials, a soft rubber gasket was placed at the top and bottom of the glass tube wall. Soft rubber gasket material was also used as spacer material between the teflon insulation block and the teflon pad on the upper end plate. All important joints were further sealed with "Plastic Rubber Cement" which is an elastic rubber in putty form and is sold by Sears Roebuck and Company. When this material dries it has the properties of soft rubber. Condensate from the condenser surface was collected at the bottom of the steam chamber. The condensate exited the steam chamber by means of a ½ inch pipe which was threaded through the bottom end plate of the steam chamber. With this valve open the condensed steam vapor was forced by chamber pressure into a 1000 ml separation funnel where the condensate rate was measured.

Steam entered the chamber through the center access hole in the glass chamber wall. The holes (see figure 2.4) were used to vent steam from the chamber. The second hole from the top of the glass tube was used to insert a pressure probe into the steam chamber. The access holes were sealed by rubber stoppers. Each steam chamber probe was sealed into a hole drilled through a rubber stopper. The stopper was then forced into one of the holes in the glass wall of the steam chamber. This method for gaining access to the inside of the steam chamber provided a steam tight seal.

Water entered at the top of the test section and exited at the bottom. A 1 inch O.D., 6 inch long copper tube was soldered into a brass fitting which had external one inch pipe threads (see figure 2.3). This assembly was then screwed into the water passage of the condenser surface which had been taped for a 1 inch pipe thread on both ends. The test assembly was connected to the main water lines with flexible rubber hose.

Water was pumped through the test section by a closed loop system. Figure 2.5 shows a schematic of the water loop. No data was taken from the water loop since its only function was to provide a controlled temperature heat sink. The water loop was designed to provide high and very steady flow rates without causing mechanical vibration of the test section. The only instrumentation in the water loop was a Fisher-Porter Rotometer flow meter and a pressure gage to indicate the magnitude of the pump head. The centrifigal pump was driven by a 7½ horsepower General Electric variable speed direct current motor. The direct current was supplied to the motor by a motor-D.C. generator set. The pump unit was equipped with a separate control panel with a variac dial to control the pump motor speed. The pump speed was varied to give minimal temperature variation of the cooling water while it passed through the test section. Water was pumped from and returned to an open galvanized tank which

had a 50 gallon capacity. The large capacity of this tank reduced the effect of temperature and pressure variation in the water loop to a minimum. The water temperature in the tank was allowed to increase by passing it through the test section where it absorbed heat from the condensing steam. When the tank water reached a desired temperature, cold tap water was introduced into the tank. The cold water stabilized the tank water temperature. The tank was equipped with an overflow drain which allowed the excess water to leave, keeping the volume of water in the water loop constant. The cooling water was taken directly from the tap as it was supplied by the City of East Lansing.

The steam used in this research was taken directly from the steam lines supplied by the Michigan State University power plant. Since the teflon film used to promote dropwise condensation is not effected by small traces of impurities in the steam, no attempt was made to purify the steam before it entered the test section. Before entering the test section, the steam was passed through a small moisture separating tank that also acted as a heat exchanger to remove any superheat. The steam entered the test chamber in approximately a saturated state. Both the temperature and the pressure of the steam were measured in the test chamber. A special diffuser manifold allowed the steam to distribute to all parts of

the chamber without causing undesirable vapor velocities over the condenser surface. The steam was experimentally stagnant at the condenser surface.

A chemical analysis of the boiler feed water used to produce the steam is presented in tables I and II in appendix IV. Tables I and II are the results of tests made by the Allis-Chalmers Manufacturing Company of Milwaukee, Wisconsin on May 11, 1965. The feed water used to produce the steam used in this research had a total of 1.8 mineral parts per million parts of water. There were less than five parts per million of dissolved oxygen in the feed water.

All temperature measurements were made with thermocouples. The thermocouples were made from 24 gage (GG-24-DT) fiberglass covered copper constantan wire. This wire was supplied by The Thermo Electric Company of Saddle Brook, New Jersey. The thermocouple beads were made by placing twisted ends into a gas flame until the two wires fused into a small metalic ball. The thermocouples made in this manner were calibrated at the ice point and at the steam point. The primary temperature recording instrument was a model 8686 millivolt potentiometer made by the Leeds and Northrup Company. The error in temperature measurement introduced by the recording instrument was less than $\pm 0.046°F$ at 200°F. A complete

analysis of the errors involved in the test section is presented in appendix II.

An 8 point Brown Electric Automatic Temperature Recorder manufactured by the Minneapolis Honeywell Company was also used. This instrument was used to determine when the system reached a steady state condition. No recorded data was measured with this device.

The thermocouples which were imbedded in the copper test section were constructed as follows. The thermocouple leads were drawn through a 5/32 inch O.D by 9/16 inch long piece of stainless steel tubing. The bead of the thermocouple was allowed to extend out of the end of the tube a distance equivalent to the diameter of the bead. The tube was then filled with an epoxy that was allowed to harden. The excess epoxy was then cleaned from the thermocouple bead and the entire assembly was forced into the ½ inch deep holes drilled in the ends of the copper cylinder (see figure 2.3). Since the stainless tubes had a slightly larger outside diameter than the holes in the copper cylinder, the probes had to be inserted with force until the thermocouple bead was forced against the copper. Care was taken during each step to insure that the thermocouple had not been broken during insertion. With the thermocouple firmly in place the outside interface between the copper and the stainless steel

tube was cleaned with sandpaper and covered with a small quantity of epoxy. With all eight thermocouples so placed the copper cylinder was heated with forced hot air. The thermocouple positions were then checked to insure that they were giving proper readings. With the thermocouples thus placed the copper cylinder condenser section was assembled with the teflon guard insulations to allow the lead wires of the thermocouples to pass inward to the 1 inch copper water passage tube and then out of the test section. The thermocouple leads were connected to a selector switch on the test console. This switch allowed the potentiometer to be connected with any thermocouple circuit in the system. All thermocouple circuits were carefully labeled to establish their location in the system.

2.2 HEAT TRANSFER EXPERIMENTAL PROCEDURE

The heat transfer experiment was designed to measure the following quantities;

1. Condenser surface temperature at four locations.
2. Temperature at four locations in the copper test cylinder one inch behind the condenser surface.
3. Temperature of the steam in the test chamber.

4. Pressure of the steam in the test chamber.

5. Condensing rate of the steam.

Figure 2.5 shows a schematic drawing of the entire test apparatus. The following discussion will make frequent reference to the information presented in figure 2.5. Before the steam chamber was assembled the teflon condenser surface was washed with a mild detergent to remove any grease and finger prints that may have been on it. The surface was then rinsed with distilled water and allowed to dry in the room air. The condenser test chamber was then assembled and no further cleaning of the condenser surface was made during the experiment. The following procedures were followed during each experiment.

1. Valve number 1 was opened to allow steam to enter the system from the main steam line.

2. Valves 3, 4, 5, 6, 7 and 13 were fully opened to allow steam vapor to vent from the test section.

3. Valve 2 was then opened slowly to allow steam to enter the test section. Enough steam was let in to create a small positive pressure (1 inch of Hg or less) in the steam chamber.

4. Steam was allowed to vent through valves 3, 4, 5, 6, 7, and 13 for at least 1 hour before taking data to insure that all the entrap-

ped air had been removed from the test chamber.

5. Valves 8 and 9 were then fully opened in the water loop and the pump was started. Water was circulated (at about 35 GPM) through the test section while valve 2 was regulated to insure that the steam chamber pressure remained positive. The water was allowed to circulate and be heated by the condensing steam vapor until a desired condenser surface temperature was reached.

6. Upon reaching the required temperature, cold tap water was introduced into the reservoir tank by opening valve 11 enough to stabilize the cooling loop temperature.

7. Vent valves 3 and 13 were then closed and the rate of venting from valves 6 and 7 was reduced to minimize the effect of vapor velocity in the test chamber. Valve 2 was also adjusted at this point to stabilize the steam chamber pressure. The steam chamber pressure was always maintained at between 2 and 3 inches of Hg above atmospheric pressure.

8. The temperatures in the test cylinder were then monitored on the automatic temperature

recorder until the system reached a thermal steady state condition.

9. When a study state had been established valve 5 was closed and the time required to collect 1000 millileters of condensate was measured.

10. While collecting condensate the various thermocouple circuits were switched into the Leeds and Northrup Potentiometer and the temperature data was recorded.

11. After the data had been recorded valve 5 was reopened to allow the condensate collector to empty.

12. Steps 9, 10 and 11 were always carried out at least twice to insure that the data was not changing with respect to time.

13. Valve 11 was adjusted to establish a new condenser surface temperature and steps 6 through 12 were repeated for the new data point.

It should be noted that minor adjustments were sometimes made in the cooling water flow rate to reduce the temperature variation as it traversed the test section. As a rule the flow was kept as high as possible without causing undesirable vibrations of the test section.

A test was made to establish the rate of condensate from the inside of the glass wall of the steam chamber. During this test the steam chamber was not connected to the water loop. By forcing hot air through the cooling passage the condenser surface was raised to a temperature above the steam saturation temperature. Condensate was then collected off the glass wall of the steam chamber. Assuming that this rate of condensation represents a constant, one could subtract it from the condensate rates measured during a heat transfer test. It was found that the rate of condensation from the walls of the steam chamber was less than 1.0 percent of any condensate rate measured during a heat transfer test. Since this effect was small, no correction was made in the condensate data.

3.0 RESULTS OF THE HEAT TRANSFER EXPERIMENT.

The original data for the heat transfer during dropwise condensation are presented in appendix I. Figures 3.1, 3.2, and 3.3 present the data graphically.

The heat transfer coefficient for dropwise condensation on a teflon surface was determined over a range of $(T_{sv}-T_s)$ of 0.5°F to 7.4°F. An analysis of the experimental error that is inherent in the data is presented in appendix II. Sample calculations indicating the procedure used to reduce the data are presented in appendix III.

The heat flux data is graphed as a function of $(T_{sv}-T_s)$ in figure 3.1. The data from this study is compared with data by Welch(10). The data are shown to be in rather good agreement. Welch used two different condenser surfaces. One was a ¼ inch vertical copper slab and the other was 7 7/8 inch vertical copper slab, on which cupric oleate was used as the promoter. The wide variation of condenser surface height used to produce these data indicates that dropwise condensation is not influenced by this parameter, at least up to the one foot high surfaces used during this program.

The heat transfer coefficient data is presented in figure 3.2 where it is compared with data by Welch(10) and Reisbig(1). The agreement between the three sets of

Figure 3.1, Heat Flux Data Correlation

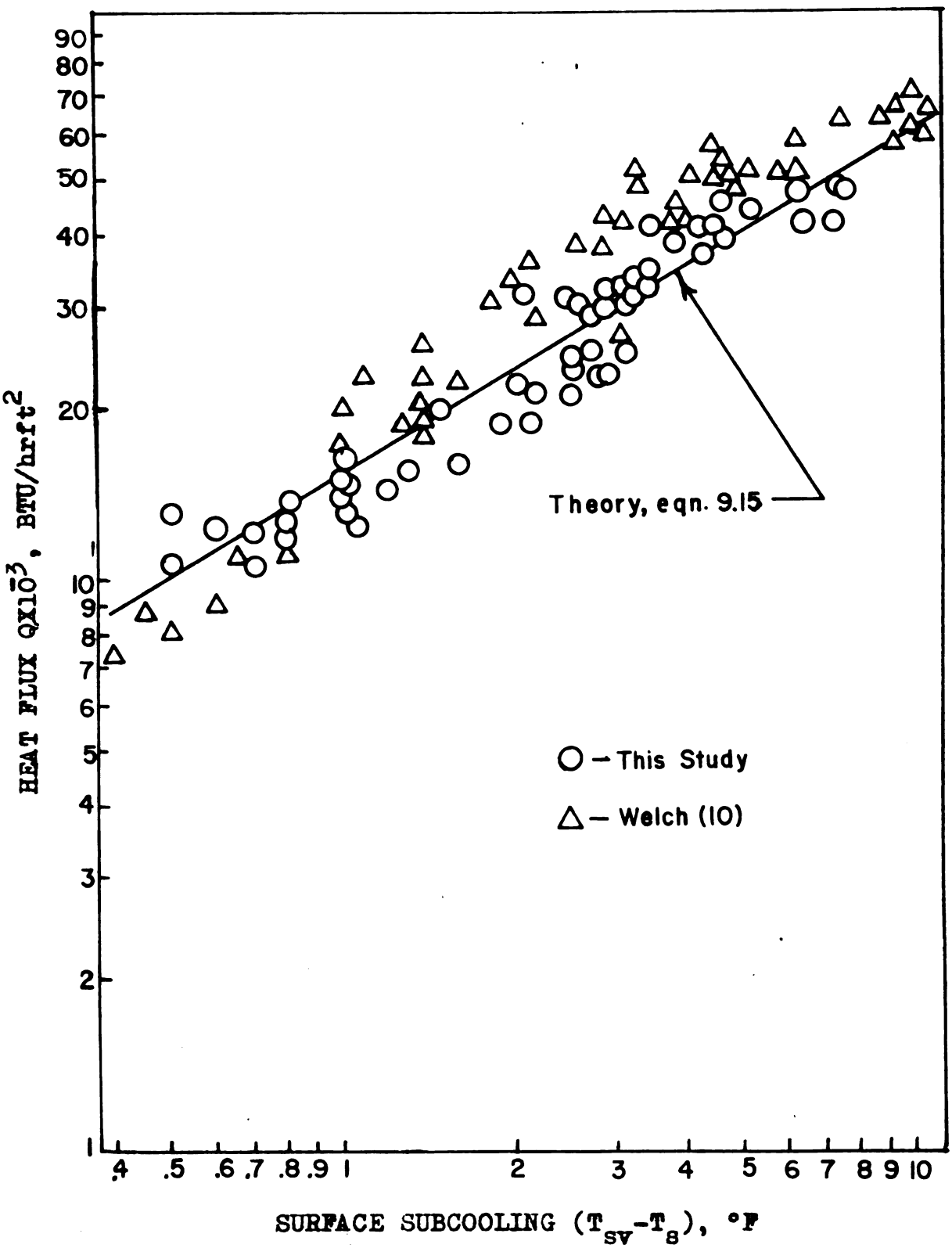

data is again quite good. Welch's data is higher in the range of $(T_{sv}-T_s)$ from 1°F to 3°F. This is most likely due to the experimental method used by Welch to determine the heat flux. His heat flux values were based exclusively on temperature measurements. His ¾ inch high condenser surface, which was used to obtain most of the data in the range mentioned, had a wall thickness of several inches. Any heat leak from the edge of the condenser surface would result in a higher measured ΔT and thus a higher flux caused by this experimental error.

The data derived from the present research is believed to be more reliable since the condenser surface was much larger, thus reducing the effect of heat leakage from the system. Also, two independent sets of data were taken for the heat flux to insure reliable results.

The data from reference (1) is shown to extend the range of the present data and to have a good linear relationship to the data from this program. Reisbig(1) used a ½ inch O.D. horizontal tube which was coated with a thin film of teflon. The effect of condenser geometry again seems minimal since the data taken from a horizontal tube correlates with the data from the one foot high vertical condenser surface used during this program.

The theoretical curves shown in figures 3.1 and 3.2 are the result of equations whose complete derivations

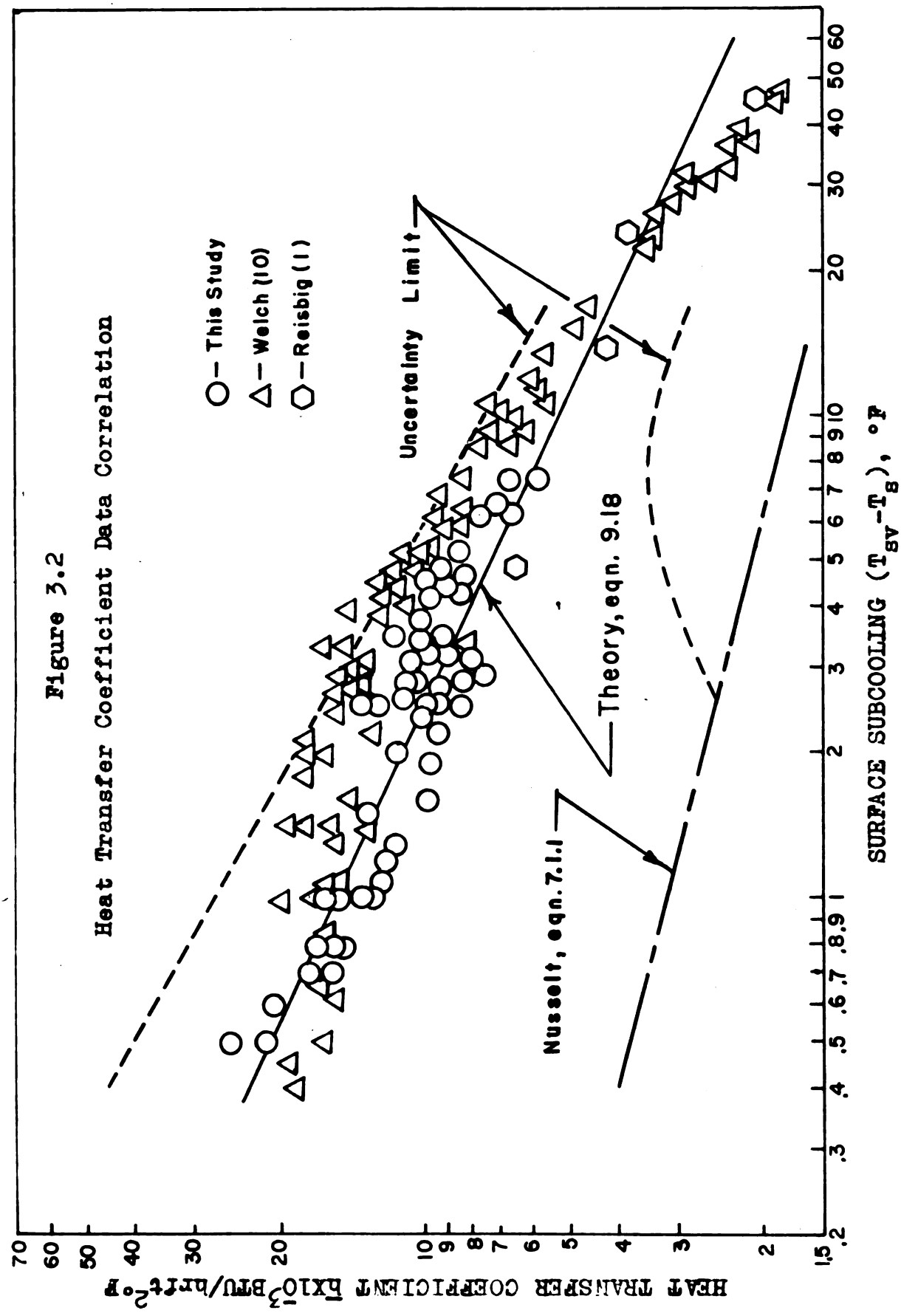
Figure 3.2
Heat Transfer Coefficient Data Correlation
O— This Study
Δ— Welch (10)
⬡— Reisbig (1)
Uncertainty Limit
Theory, eqn. 9.18
Nusselt, eqn. 7.1.1
HEAT TRANSFER COEFFICIENT h x10⁻³ BTU/hr ft² °F
SURFACE SUBCOOLING ($T_{sv}-T_s$), °F
70
60
50
40
30
20
10
9
8
7
6
5
4
3
2
1.5
.2
.3
.4
.5
.6
.7
.8
.9
1
2
3
4
5
6
7
8
9
10
20
30
40
50
60

are presented in section 9.0. A complete discussion of the correlation between the data and the theoretical equations is also referred to section 9.0.

Figure 3.3 shows the heat transfer coefficient plotted as a function of heat flux. A number of authors (35, 39, 40) have indicated that the heat transfer coefficient is independent of heat flux. Shea and Krase(14) show that there is some variation of h with Q . The data from this program is compared with data by Fatica and Katz(9), Reisbig(1) and Welch(10). The data from this program as well as references (9, 1) indicate a strong downward trend for h as Q gets larger. Figure 3.3 shows that the scatter in the data for this type of correlation is quite large. Welch's data shows a reasonable agreement with the data from this program, but it has a larger degree of scatter. The data of Fatica and Katz(9) shows no trend by itself, however, it groups into the data from this program. The data by Reisbig(1) follows the trend of the data from this program but it is located in the lower portion of the data envelope. Due to considerable data scatter the exact location of the data curve is difficult to determine. The solid line represents a reasonable correlation if most of Welch's data is ignored. The two dotted lines represent the general shape of the upper and lower bounds of the data envelope. The general conclusion drawn from figure 3.3 is that the heat transfer

Figure 3.3

The Dependence of Film Coefficient

On Heat Flux During Dropwise Condensation

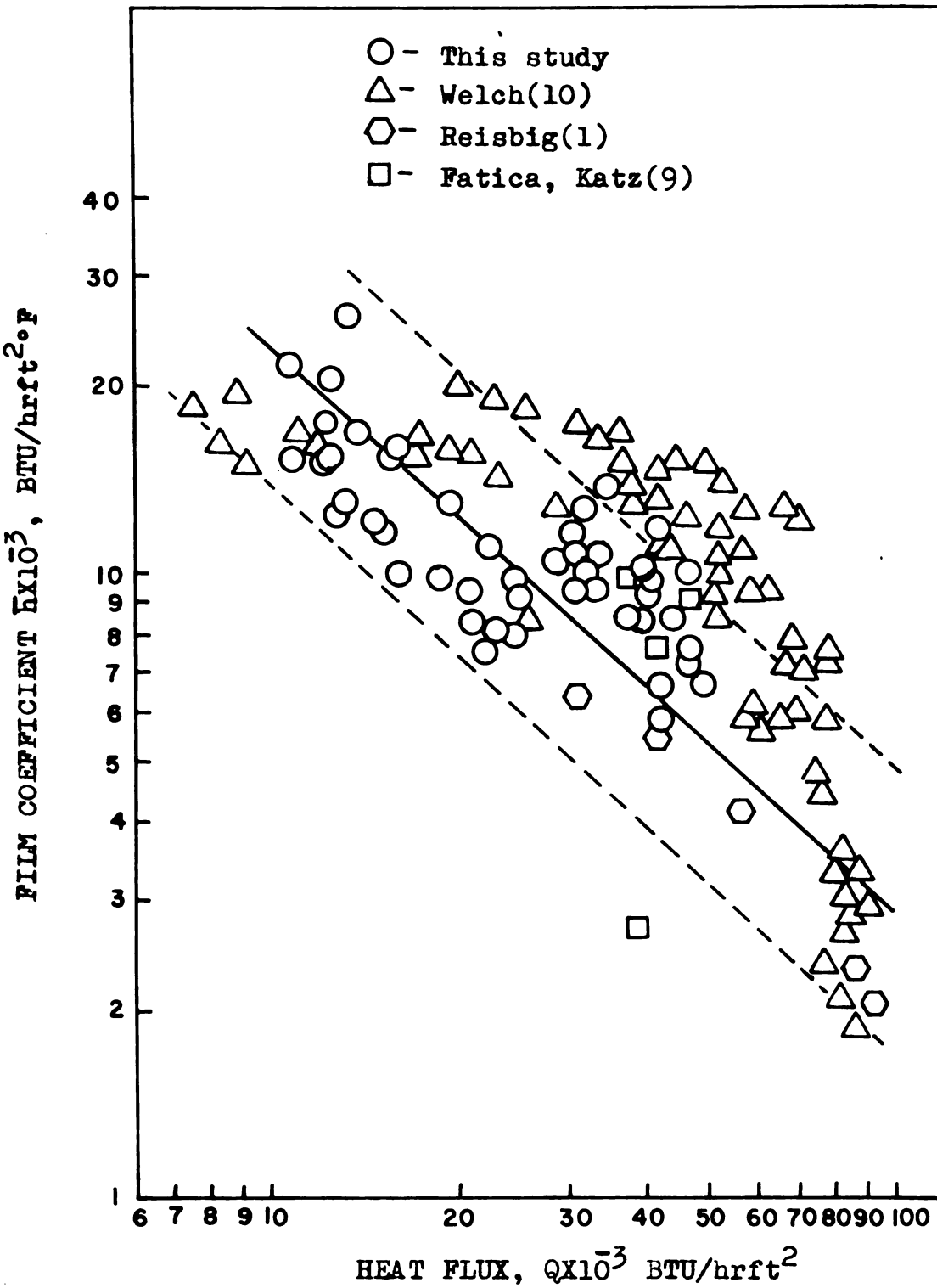

coefficient is a dependent function of heat flux during dropwise condensation. The heat transfer coefficient decreases as the heat flux increases. It is reasonable to assume that the heat transfer coefficient would decrease until a point is reached where it is equal to the value derived from filmwise condensation. Any heat flux beyond this point would only produce filmwise condensation. This can be visualized if one considers that at this high heat flux the drops would try to develop so rapidly that a continuous condensate layer would form on the condenser surface. The heat flux at which this would occur would take place at a very large value of $(T_{sv}-T_s)$.

4.0 THE PHOTOGRAPHIC EXPERIMENT

A series of high speed motion pictures were taken during controlled heat transfer experiments. High speed 16mm motion pictures were taken of the entire length of the condenser surface and also through a microscope which was focused on the condenser surface. The pictures were taken at film speeds in the range of 720 to 2500 pictures per second and over a range of 1.0 to 3.4°F temperature difference between the saturated vapor and the condenser surface ($T_{sv}-T_s$). The photographic experiment was designed to supply data of a qualitative and quantitative nature. A number of still photographs were also taken of the condenser surface during dropwise condensation for low values of ($T_{sv}-T_s$).

4.1 PHOTOGRAPHIC APPARATUS

The photographic apparatus and heat transfer apparatus were shown together in figure 2.1. Figure 2.2 shows the location of the microscope in relation to the condenser surface.

The motion picture camera used in this experiment was a 16mm Wollensak Fastax, Model WF3. This camera is capable of a maximum film speed of 8000 frames per second, and a minimum film speed of 150 frames per second. The

shutter operation in this camera is provided by a rotating square optical glass prism. The image formed by the lens system at the film plane is moved in synchronism with the film on the sprocket by this rotating prism. At the top nominal speed of 4,000 frames per second the exposure time per frame in this system is 1/20,000 second.

The fastax WF3 uses 100 foot reels of film. The film used was Kodak Tri-X reversal movie film. Timing marks were placed on the edge of the film while taking pictures by a neon glow lamp which was focused onto the edge of the film. The lamp was energized by a 110-volt, 60-cycle power source which produced 120 flashes per second, which is equivalent to a time interval of 0.00833 seconds between the start of successive flashes. The camera was mounted on a tripod and could be used with one of its lens assemblies or connected to a Zeiss microscope. The microscope was mounted on an independent assembly that allowed it to be adjusted up and down, depending on the location on the condenser surface that was to be observed.

When pictures were taken of the entire length of the condenser surface, the camera was used alone with its 35mm f/2 Raptar lens. For this type of picture, lighting was provided by two 150W Sylvania spot lamps, each placed about one foot from the subject.

When pictures were taken through the microscope the camera's 35mm f/2 Raptar lens was used on the camera. The camera was then moved into alignment with the eye piece of the microscope. The magnification provided by this system was varied by changing the eyepiece lens in the microscope. Magnifications as high as 18.5X on the film were obtained by this system. The light source used to give the microscope pictures was provided by two Bausch and Lomb 115v A.C. motor driven carbon arc lamp projectors. Each of these lamps was provided with a lens system which allowed the light to be focused onto a spot about ¼ of an inch in diameter. The projected light was passed through filters and a water wall to remove as much of the long wavelength, high energy radiation as possible. Light produced in this manner provided a subject so bright that it could not be observed through the microscope with the naked eye. In fact, it was possible to project the image onto a screen using the lens system in the microscope as a projector. The objective lens in the microscope was a Carl Zeiss Jena with a focal length of 5.3mm and a numerical aperature of 0.14. The numerical aperature of the objective lens controls the resolving power of the optical system. A given objective lens is capable of resolving specimen structure which is separated by a distance $\frac{W}{2\ N.A.}$, where W represents the wavelength of the illuminating light. Light from a carbon

arc has a characteristic wavelength of about 5500A (0.000022 inch), thus two lines separated by a distance of approximately 0.00008 inch (2 microns) can be resolved by the objective lens used in this research. This was enough resolving power to meet the objectives of the experiment. The depth of focus provided by the objective lens was $\pm$0.002 inch.

Still photographs were taken with a Zeiss single lens reflex camera equipped with a 50mm f/2.8 lens system. The 35mm negatives were produced with Kodak Tri-X Pan Film (ASA 400).

4.2 PHOTOGRAPHIC EXPERIMENTAL PROCEDURE.

The procedure for starting the heat transfer equipment and for establishing a data run is described in section 2.2. Once the required heat transfer data had been established, the microscope was raised into position to observe a section of the heat transfer surface. A Sylvania 150W spot lamp was used as a light source while adjusting and focusing the microscope. With the microscope in position the two Bausch and Lomb carbon arc light sources were positioned and focused onto a spot on the condenser surface in front of the objective lens of the microscope. Next the movie camera was moved up to the apparatus and aligned with the microscope. The 35mm

f/2 Fastax Raptar Lens was used in the camera. With this camera lens system placed about ½ inch away from the eyepiece of the microscope, it was possible to focus the combined camera-microscope lens system such that a perfect image of the condenser surface was formed at the film plane in the camera. The camera lens was opened to the maximum f/2 setting and the focusing scale was set at infinity. The microscope was first focused to give a clear eyepiece image; the camera was then focused through an integral reflex-type view finder. Rough focusing of the camera was obtained by moving the camera and tripod toward or away from the microscope. The camera's view finder was equipped with a parallax recticle. By moving an eye from side to side, and if the subject moves with respect to the rectile, the picture is not in focus. Adjustment of the focusing knob on the front lens of the camera was used to eliminate the parallax, and thus bring the microscope image into focus. Fine adjustment of the microscope was all that was needed at this point to bring the camera-microscope system into sharp focus.

Focusing was further directly checked by inserting a piece of ground film on the drive sprocket of the camera. By placing a dental minor into the camera the subject image was observed on the ground film.

The camera was set to give the desired film speed,

and the 100 foot reel of film was placed into the camera. The glass wall of the steam chamber was defogged by a hand held hot air blower. When defogging was completed the carbon arc light sources were started and the pictures were taken.

The procedure for taking pictures without the microscope was the same except the light source for these pictures was supplied by two 150W Sylvania Spot Lamps placed about one foot from the subject.

The procedure for taking still pictures through the microscope was the same as above. The light source for these pictures was supplied by the two carbon arc lamps.

For all photographs the proper film speed or shudder speed was determined by developing short strips of film in the mechanical engineering darkroom. This trial and error procedure was continued until the proper exposure was obtained.

The movie film was processed commercially by Capital Films Inc. of Lansing, Michigan.

The degree of magnification of the optical system was measured as follows. A stage micrometer was used as the object. The divisions on the stage micrometer were 0.01mm. The camera-micrometer optical system was focused

onto the stage micrometer and the width of the field of view could easily to correlated to the width of the film negative. To get the number of diameters of magnification at the film plane one divided the negative width by the reading taken from the stage micrometer. Any discussion of magnification in this report will be taken as meaning the number of diameters of magnification on the film negatives.

5.0 RESULTS OF THE PHOTOGRAPHIC EXPERIMENT.

The data associated with the high speed 16mm motion pictures is presented in appendix I. A total of twenty (one hundred foot) reels of film were taken. These pictures were used as follows,

1. To provide qualitative information to aid in the formulation of a mechanism theory for dropwise condensation.
2. To provide quantitative information to establish the magnitude of parameters associated with the mechanics of dropwise condensation.

The films indicate that the condensation process takes place in very small drops (a few microns in diameter or less). The smallest drop that could be clearly observed had a diameter of about 0.0001 inch or about 3 microns in diameter. It was evident that drops of this size and larger were only able to grow by combining with other drops. This indicates that drops larger than a few microns do not grow by capturing significant quantities of vapor molecules. This also indicates that the larger drops function as condensate reservoirs that collect and store liquid but do not contribute to the heat transfer process. Once a reservoir drop is established the surface under it is inactive to heat transfer. The

coalescence of drops creates bare surface and thus active heat transfer area is produced. The process of growth continues until a drop either gets large enough to slide down the surface, or the drops are swept down the surface by a drop which has rolled over the area from above. Thus active heat transfer surface is continually created by drop coalescence with other drops and by drop roll-off.

The drop field grows in a rather orderly fashion. The first drops that appear in the films (0.0001 inch diameter) are closely packed and of uniform size. Each time a series of coalescences takes place, the newly created larger drop field is less closely packed but still of rather uniform size and distribution. The bare areas between the newly formed drops fills in with smaller drops which collide with and feed the larger drops. This process continues until at roll-off there are drops of all intermediate diameters on the surface. The sequence of events just described is illustrated by the series of pictures presented in figure 5.1.

The coalescence between water drops is a very rapid phenomenon. For drops of comparable size the coalescence time is less than 0.001 seconds. If one drop is significantly larger than the others, the process takes place with even greater speed. On the average about 3 comparable sized drops combine during a given coalescence.

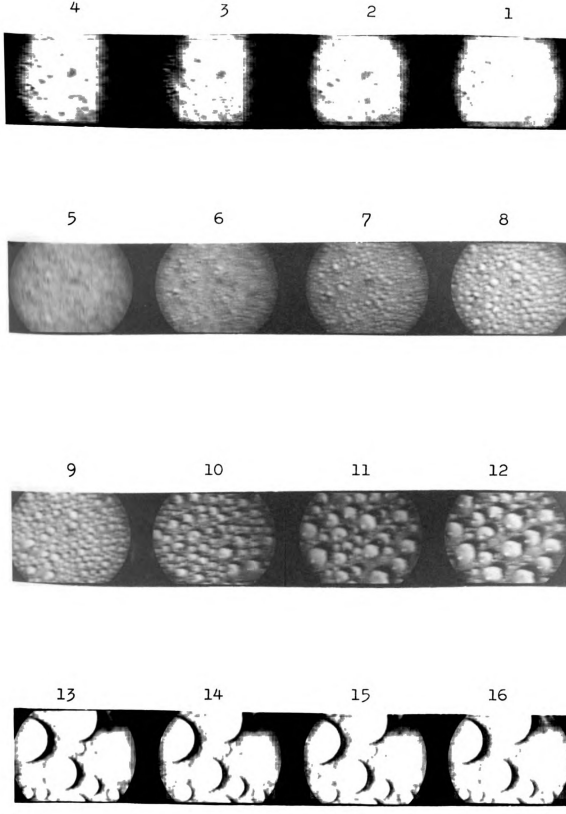

Figure 5.1 Sequence of Pictures Showing Drop Field Build up

Rapid coalescence indicates that condensate viscosity does not have a strong effect on the dropwise condensation phenomenon associated with water vapor. The speed of coalescence is controlled primarily by capillary forces. This observation will probably be true for other fluids which can be condensed in a dropwise fashion, however, this will have to be proven with further research.

Another phenomenon not visible to the naked eye occurs when a drop rolls down the condenser surface. When the drop first starts to slide it is in the approximate shape of a hemisphere. As it progresses a comet like tail extends out behind the drop. By the time the drop reaches the bottom of the one foot condenser surface the tip of the tail had a tendency to fracture away and stop in the middle of the roll-off track. The following sketch illustrates the process being discussed.

drop at start of roll-off

drop after traveling 6 inches

drop after traveling 12 inches

This phenomenon may effect the heat transfer rate when long (greater than one foot) vertical condenser surfaces are considered. The tail fragments deposited in the roll-off track would reduce the heat transfer rate since the

amount of active surface area would be less.

The fact that roll-off drops achieve sizable velocities is shown in figure 5.2. The velocity data used in figure 5.2 was obtained from low magnification high speed movies by analyzing the motion of a drop over a distance of about 3 inches measured at the top, center and bottom of the condenser surface.

When the drops reached a diameter of about 0.1 inch the roll-off process started. The roll-off track width remained about 0.1 inch for the entire length of the condenser surface. Almost all roll-off drops occured within 1 inch of the top of the condenser surface.

The growth rate due to drop coalescence is presented in figure 5.3. The growth rate is shown to be a strong function of the degree of surface subcooling ($T_{sv}-T_s$). The growth rate at a point 5 inches below the top of the condenser surface is shown to be different from the growth rate at 9 inches. This can be explained by the fact that the ($T_{sv}-T_s$) value associated with each curve represents an average of the temperature measurements taken at the top and bottom of the condenser surface. Since there was as much as a 2°F differential in the surface temperature between the top and bottom, the lower points were experiencing a lower actual ($T_{sv}-T_s$) than points higher on the condenser surface. This again shows that drop growth

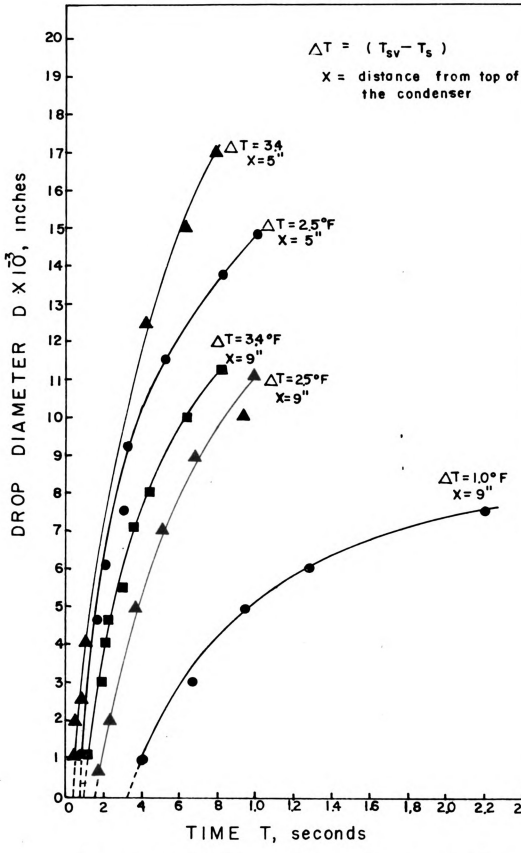

Figure 5.3 Effect of T_s on Drop Growth Rate.

Figure 5.2 Roll-off Drop Velocity

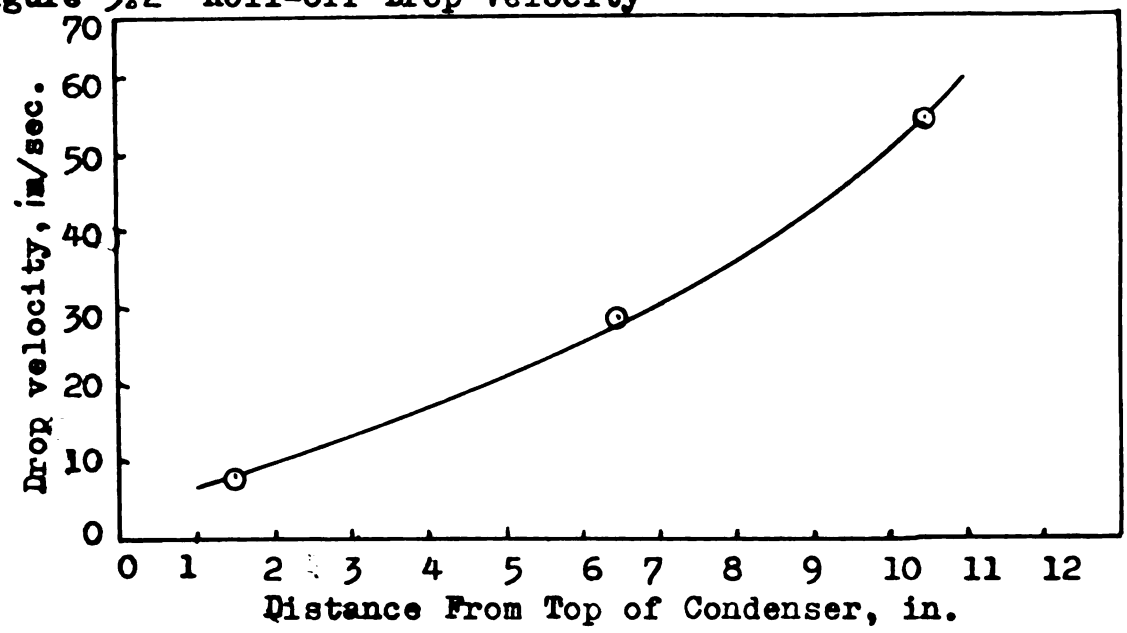

Figure 5.4 Effect of Temperature On Maximum Drop Size

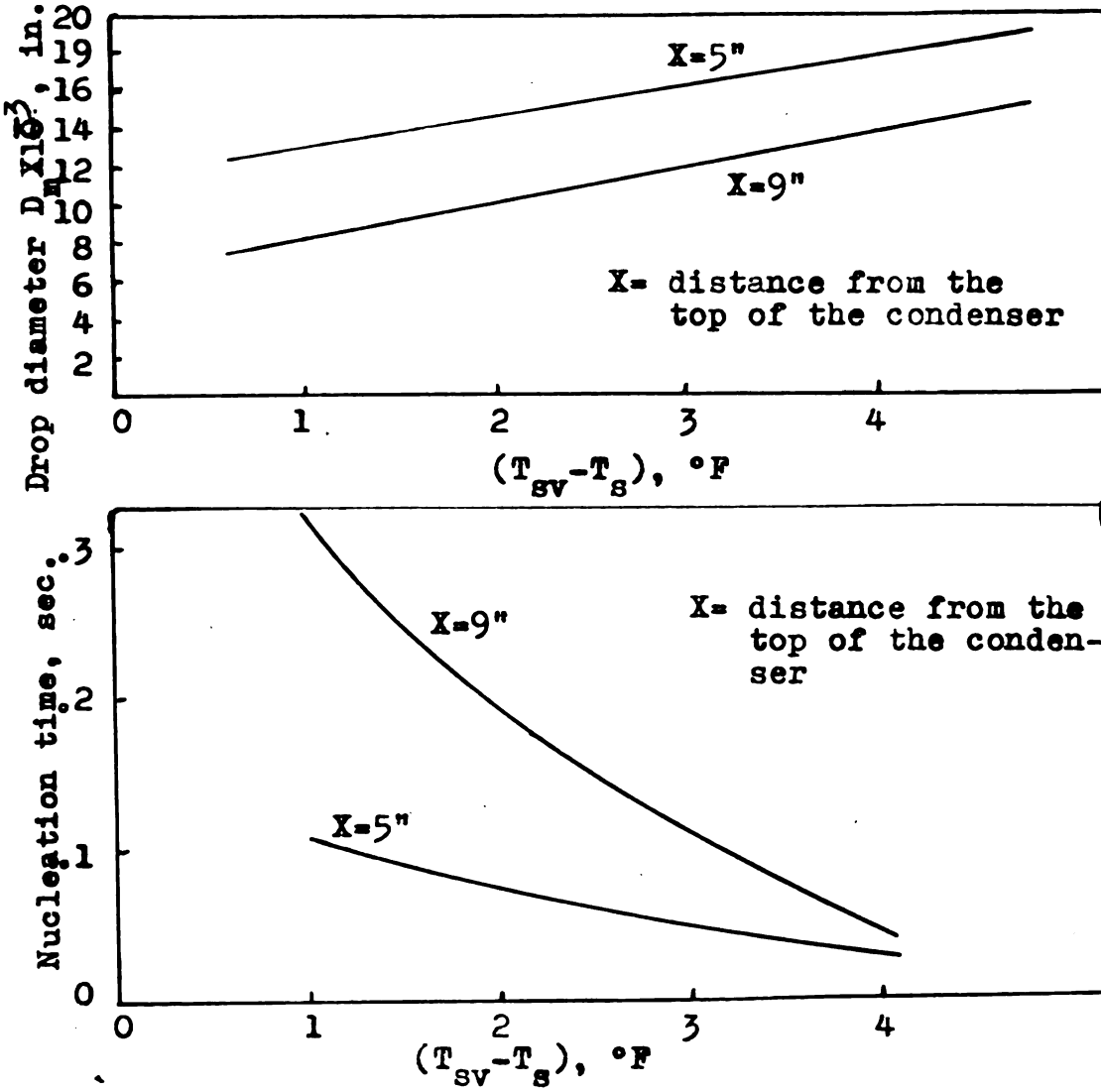

Figure 5.5 Effect of Surface Temperature On Drop Nucleation

rate is very sensitive to small changes in $(T_{sv}-T_s)$.

The right hand end points on the curves in figure 5.3 represent the average maximum drop size just before the surface is swept clean by a roll-off drop from above. Figure 5.4 shows the average maximum drop size at three points on the condenser surface as functions of $(T_{sv}-T_s)$.

By extrapolating the left hand end of the curves in figure 5.3 to the time axis it is possible to estimate the nucleation time at two points on the condenser surface as a function of $(T_{sv}-T_s)$. The results of this procedure are presented in figure 5.5.

The assumption that condensate drops nucleate is discussed in detail in sections 7.0 and 8.0.

The conclusion that heat is transferred almost entirely through microscopic drops that nucleate on the condenser surface is used in section 8.0 to develop a complete theory for the mechanism of dropwise condensation. These observations are also used in section 9.0 as a basis for a mathematical model which is used to formulate an equation for the heat transfer coefficient.

6.0 THE PROMOTER OF DROPWISE CONDENSATION.

Dropwise condensation of water vapor is not a natural phenomenon on most chemically clean metalic surfaces. To bring about dropwise condensation, a non-wetting agent must be introduced at the condenser surface. This agent can be any substance which will adhere to the metalic surface and which will not allow the condensate to wet this surface. Any substance that causes dropwise condensation of a vapor is called a promoter. The promoter used in the experimental phases of this program was a thin film of teflon which was coated onto the condenser surface.

Teflon is the registered trademark for a family of Dupont fluorocarbon resin products which are either tetrefluorethylene resins (TFE-resins) or fluorinated ethylene propylene resins (FEP-resins). The resin used in this study was of the TFE-resin type which is designed throughout the discussion as teflon.

Before going on with a discussion of the promoter used during this program it will be instructive to consider some promoter schemes used in the past. A few of the better steam promoters have been fatty acids such as oleaic or stearic acid, mercaptons (benzyl) and various waxes and oils. These chemicals are either painted onto the condenser surface or added to the boiler feed water.

In the second case it is important that the promoter condense first to form a nonwetting film. Welch(10) reports continuous dropwise condensation for 10,000 hours by using cuprus oleate on a pure copper condenser surface. A significant property of chemical promoters is that they become ineffective in a matter of minutes if oil, rust or some other impurity is present in the vapor. Industrial condensers do not work with the degree of purity required by most chemical promoters. Since these promoters will not work in a "dirty" environment the benefits of dropwise condensation have not been exploited. Even if present chemical promoters worked well with dirty steam, copper condenser surfaces would have to be used exclusively. This fact alone is a severe restriction to the design engineer when weight and/or strength are prime considerations. The ideal practical promoter should function for extensive periods of time (a year or more) and not be effected by a reasonable degree of vapor impurity. A promoter should also work well on metal surfaces commonly used in the design of steam condensers, such as stainless steel and aluminum. The need for a reliable dropwise promotion method is clearly indicated in the 1961 issue of a United States Department of Commerce Bulletin entitled, "Inventions Wanted By The Armed Forces And Other Government Agencies". On page five of this article the following is printed,

"1561. MATERIALS TO INDUCE DROPWISE CONDENSATION. Coatings or materials which will induce dropwise condensation on condenser surfaces and be effective indefinitely. The present dropwise promoters do not last for a long period of time."

The utility of using a thin film of teflon as a scheme for promoting dropwise condensation on horizontal tubes was reported by Reisbig(1). In that research a 0.00025 inch thick film of teflon was coated onto a ½ inch O.D. aluminum tube. It was shown that a teflon coated (0.00005 inch thick) tube would experience a heat flux twice as great as an uncoated tube under the same operating conditions. It was also reported that regular power plant produced steam was used and that no observable effects were produced on the ability of teflon to promote dropwise condensation for periods of time up to 100 hours.

Teflon is a fluorinated derivative of polyethylene. Teflon is produced by replacing hydrogen atoms in the ($-CH_2-$) radical by fluorine atoms to form a new ($-CF_2-$) radical. This fluoridation process produces a drastic effect on the properties of the compound. The new material becomes chemically inert, is not wetted by most solvents and has no ability to absorb water. Each of the above stated properties are important features of a good

dropwise condensation promoter. The ability of teflon to adhere to metalic surfaces is an important consideration. Since teflon is inert, a chemical bond is not possible. This leaves only a mechanical bond to keep the thin deposit in place on the condenser surface. It has been found (1) that teflon bonds very well to metals whose oxide are tough and adheres to the parent metal. Teflon adheres very well to aluminum surfaces. This is most likely due to the fact that aluminum oxide is porous and forms a very strong bond to the parent metal. The teflon fills these pores, and thus anchors itself in a strong mechanical fashion to the aluminum surface. Metals like copper and iron should be more difficult to coat with teflon since their oxides are very loose and tend to crumble. From a heat transfer point of view, teflons low thermal conductivity is a most undesirable feature. If thick (more than about 0.001 inch) films of teflon are added to a condenser surface, the thermal resistance introduced will cancel out the effects gained by dropwise condensation. This means that a teflon film should be about 0.0005 inches or less thick to be effective. Topper and Baer(2) report durable teflon films as thin as 0.0001 inch. The production of very thin teflon coatings and/or methods of improving their thermal conductivity should be the object of future research projects. The thickness and thermal conductivity of the

ultimate teflon coating are controlling parameters in the determination of the dropwise heat transfer rate.

To better understand the physical and chemical nature of polytetrafluoroethylene, a short discussion of this topic is in order. An understanding of the chemical behavior of fluorinated compounds will point out the difficulty of inventing an ultimate coating for use as a promoter. The basic problem of producing an ultimate coating is controlled by chemical and process oriented considerations. Thus, the invention of an ultimate fluorocarbon promoter is a problem to be considered by industries engaged in fluorine chemistry research.

Fluorine is the most reactive element known to man. This is clearly demonstrated by its ability to oxidize materials such as glass or metal. Many of the physical properties of the class of fluorinated compounds known as fluorocarbons can be related to the nature of the C-F bond. For a better understanding of this phenomenon, a consideration of the carbon fluorine bond is presented below. As pointed out in reference (6), a simple model of the C-F bond can be constructed which shows a compact shell of fluorine valance electrons that are hard to distort from their ground configuration. When considered together with fluorines small atomic radius, the short distance between F and C in the bond, and the high

bond dissociation energy, one notes a very stable substructure which, when multiplied many times, as in a highly fluorinated compound, gives rise to the desirable properties of the fluorocarbons. The fluorocarbons as a class, exhibit chemical inertness, low toxicity, low flammability, high stability and low solubility in common organic solvents. Another characteristic is low surface tension (in the range of 6 -28 dynes/cm), again a result of low intermolecular forces. When fluorocarbons are introduced into an aqueous or an organic system, the surface tension of the entire system is drastically reduced. A surface composed of closely packed CF_3 groups (see figure 6.1) has a surface energy of 6 dynes/cm and is not wetted by most organic oils. Figure 6.1 presents a number of C-F groups and gives a comparison of the critical surface tension of each group. The critical surface tension of a solid surface is defined as that value of the liquid to vapor surface tension above which a liquid will form a droplet. Shafrin and Zisman(5) point out that if each of the polymers presented in figure 6.1 is considered as a fluorinated derivative of polyethylene ($-CH_2-$). The critical surface tension decreases approximately 3 dynes/cm for each successive 25% replacement of hydrogen atoms by fluorine atoms. Noting that the following fluids have liquid to vapor surface tensions of;

Liquid Hydrogen, σ_{lv}=2.5 dynes/cm

Liquid Nitrogen, σ_{lv}=8 dynes/cm

Liquid Oxygen, σ_{lv}=15.7 dynes/cm

Water(@ 212°F), σ_{lv}=58 dynes/cm

We note that it is theoretically possible to produce dropwise condensation for cryogenic fluids. This fact may have commercial value in the production of cryogenic fluids wherein a considerable amount of condensing equipment is used. Note (figure 6.1) that teflon is capable of condensing fluids with liquid to vapor surface tensions as low as 18 dynes/cm. This indicates that a teflon surface should produce dropwise condensation of such substances as ammonia, benzene, ethyl alcohol, ethyleneglycol and any others. Note also that perfluorolauric acid is capable of producing dropwise condensation of almost any known substance. Helium, hydrogen and neon are about the only acceptions to the previous statement.

FLUOROCARBON GROUP	CRITICAL SURFACE TENSION $\frac{dynes}{cm}$ @20°C
$-CF_3-$ Perfluorolauric acid	6
$-CF_2-$	15
$-CF_3-$	17
$-CF_2$ Teflon	18
$-CH_2-CF_3$	20
$-CF_2-CFH-$	22
$-CF_2-CH_2-$	25
$-CFH-CH_2-$	28

Figure 6.1 Critical Surface Tensions of Fluorocarbons

Since most organic compounds have a low thermal conductivity it seems apparent that producing a fluorocarbon material with a high thermal conductivity might be a difficult thing to do. With fluids like water that form dropwise condensation on teflon with great ease, it may be possible to increase the thermalconductivity by mixing a metalic powder with the teflon when it is applied to the surface.

A number of patents have been granted (16, 17, 18, and 19) in connection with the phenomenon of dropwise condensation. Nagle(16) (1935) was the first to enter a patent on this topic and Vaaler(19) (1949) was one of the last attempts to patent ideas in this area. After reading these patents, it is evident that none of the ideas presented were capable of producing dropwise condensation for periods greater than a few hundred hours of continuous operation. These patents are mentioned because they include many ideas which might be useful in the development of fluorocarbon promoting techniques.

The method used to apply the teflon to the condenser surface used in this program is presented in reference (36). The teflon coatings were produced by the Cadilac Plastics Company in Flint, Michigan. The machined copper cylinders were cleaned with acetone and polished with a fine grained emery paper to remove any existing copper

oxide and then washed once more with acetone before the coating process was started. Clean rubber gloves were used to prevent finger prints on the surface during and after the cleaning process. First a thin green coating of teflon primer was applied to the surface. The coatings were applied with a DeVilbiss TGA type spray gun using a number E90 nozzle. Proper precautions were taken to keep the entire process free of dirt of any kind. The spray gun was operated without its fan and with an atomizing pressure between 20 to 40 pounds per square inch gage. The nozzle was adjusted to give a spray barely visible to the eye. This type of spray was necessary to give a film thickness of 0.0002 inch or less. The primer coating was allowed to air dry at room temperature for about twelve hours before being placed in a fusing oven. The primer coated copper cylinder was baked in a hot air oven at a temperature between 700° and 725°F for about 30 minutes. The baking process evaporates the emulsion and allows the suspended teflon particles to fuse into a continuous teflon coating. The copper cylinder was cooled rapidly after being removed from the oven. Rapid cooling is required between 700° and 400°F to give a tough amorphous type teflon coating. Slow cooling results in an undesirable weak crystalline type teflon coating.

The final coating with a brown enamel was applied in the manner described above. The final coat was dried

and baked the same as the primer coat except that the baking time was increased an additional ten minutes. The final teflon thickness of 0.0017 inches was on the condenser surface. The thickness was measured with a micrometer by measuring the cylinder O.D. before and after the coating process.

In summary, the coating process consisted of spraying the condenser surface with a teflon enamel. In this enamel tiny teflon flakes are suspended in an emulsion. After the enamel dries the coated surface is baked in a 700°F oven. During this baking the emulsion evaporates leaving melted teflon to form an uniform coating.

It should be noted that no attempt was made to produce a minimum thickness coating during this program. The teflon surface was used primarily to provide a means of studying the mechanism of dropwise condensation of water vapor without the time deterioration of the phenomenon introduced by chemical promoters.

Aside from the possible industrial application of teflon for promoting dropwise condensation, it should be noted that the teflon surface provided an excellent research scheme on which the mechanism of dropwise condensation was studied. Since the promoting property of teflon did not change throughout the test period,and since the promoting property was not observably affected

by power plant produced steam, it can be concluded that teflon eliminated variables in this research that may have been present during other investigations into the phenomenon of dropwise condensation.

In the future the study of dropwise condensation of vapors other than water vapor should be carried out. Teflon should provide the required type of condenser surface on which these studies might be made.

6.1 COLD FINGER TESTS OF THE TEFLON PROMOTER.

An effort was made to evaluate the integraty of thin teflon coatings. Teflon was coated (approximately 0.0005 inch thick) into stainless steel, aluminum and copper tubes. The coated tubes were made into six inch long cold fingers which were inserted (one each) into a 500 ml wide mouth flask. Figure 6.2 shows photographs of the cold finger test stand.

Cold tap water was forced through the cold fingers to provide the cooling. The flasks were partly filled with water and placed on hot plates. The water vapor produced in this manner was condensed when it made contact with the cold finger. The cold finger was sealed into a flask by forcing it through a rubber stopper and then forcing the stopper-cold finger assembly into the mouth of the flask. To prevent over pressurization a ¼ inch

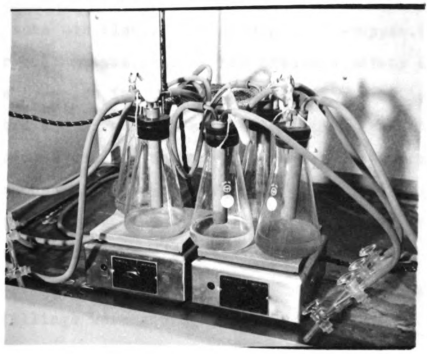

Figure 6.2 Pictures of The Cold Finger Test Devices

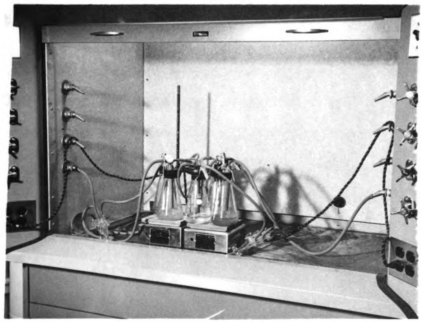

glass tube was also placed through the stopper. A small rubber balloon was used as the pressure safety device. If the pressure in the flask increased the balloon merely inflated and burst. By controlling the water flow to the cold finger and the boiling rate of the water in the flask it was possible to establish an equilibrium of the pressure in the flask. No attempt was made to eliminate air from the vapor in the flask. The water used to produce the vapor was taken from the tap. As time progressed, iron fillings were added to some of the flasks.

A total of six cold fingers were tested. There were two cold fingers for each type of metal used. The duplication was introduced to reduce the possibility of mechanical flaws in the teflon coatings. The coated cold fingers were carefully inspected for defects before and after the test period.

The cold finger tests were conducted for a total of 3080 hours of nonstop operation. The following things were observed as a result of these tests.

1. There were no failures of any of the coatings to produce perfect dropwise condensation.
2. The aluminum tube coatings were not significantly affected by the test. The only noticable effect noted on the aluminum tube coatings was a small patch of surface con-

tamination at two points on one of the cold fingers. This contamination was caused by two very small pinholes in the teflon coating. The diameter of each contaminated spot surrounding a pinhole was about 0.1 inch. Each pinhole provided a preferred condensation site. Once a preferred condensation site formed, a droplet of condensate visible to the naked eye was observed to always cover this spot. This may point out the importance of avoiding exposed metal when using teflon as a promoter. The surface contamination surrounding a pinhole was most likely produced from mineral deposits in the steam as well as aluminum oxide washed out of the pinhole. There was no evidence to indicate that the teflon film was loosing its bond to the aluminum either at or around the pinhole. There were no deviations from perfect dropwise condensation on the second aluminum tube tested.

3. The coatings on the stainless steel tubes were observed to form very small blisters at the lower end of both of the cold fingers. The blisters (about twelve in number) were only a few thousandths of an inch in diameter and were located in a horizontal straight

line. It was not observed whether or not the blisters were increasing in size, however, they were not present at the beginning of the test. Because of the similar location of the blisters on both stainless steel cold fingers, it is possible that the surfaces were not completely clean before the coatings were introduced. Although these blisters did not cause a significant failure of the condenser surface, a more serious failure of the coating may have occured if the duration of the tests had been longer. It would seem reasonable, however, that the coatings would have lasted a year or more since the area effected by blisters was extremely small.

4. Coatings on the copper cold fingers had no observable defects caused by long exposure to a steam condensing environment. From the nature of copper oxide, one might have expected a few defects on the copper tubes. Since none were observed, it might be concluded that the coatings were made without pinholes. There must also have been no dirt or oxide on the surface when the coatings were made.

It is interesting to note that during the data

collecting period the coating on the large copper cylinders were observed to form blisters as large as 0.1 inch in diameter. Three blisters of this magnitude were observed to form from what first appeared to be a very small pinhole. As in the case of the pinholes observed on the aluminum surface a mineral deposit formed in a small region around the hole. The copper surface was not able to hold the teflon around the pinhole in place and a small blister raised and filled with water. The loosening under the pinhole was probably due to the weak bond formed between copper and its oxide. This indicates that when defects do occur on a copper surface the rate of failure is much greater than in the case of aluminum or stainless steel. The large copper test section was operated for a few hundred hours in comparison to the 3080 hours duration of the cold finger tests.

The observations presented above are of a purely qualitative nature and were made to give some insight into the problems that might be encountered when using thin films of teflon to promote dropwise condensation for long periods of time. Much more research would be required in this particular area before the ultimate potential of teflon as a promoter of dropwise condensation can be determined. These tests do indicate that dropwise condensation can be maintained for very long periods of time in a rather unfavorable environment without experiencing significant failures of the promoter coating.

7.0 HEAT TRANSFER THEORIES FOR CONDENSING VAPORS.

The respective theoretical basis for the two modes of condensation is presented in this section. Section 7.1 presents a short discussion of the theory of filmwise condensation as a basis of comparison to the theoretical discussion in the sections on dropwise condensation.

7.1 THEORY OF FILMWISE CONDENSATION.

The first rigorous derivation for predicting the heat transfer coefficient for filmwise condensation was presented by Nusselt(31) in 1916. At this time Nusselt derived expressions for condensation on a vertical wall as well as for a horizontal tube. A comprehensive presentation of Nusselt's derivations can be found in references (25, 26). The general assumptions made by Nusselt are as follows;

1. The vapor condenses in a pure filmwise fashion on a fully developed liquid film.
2. Laminar flow exists everywhere within the film.
3. The vapor is stagnant or moves with very low velocities, such that the momentum and shear forces can be neglected at the liquid-vapor interface.
4. The condensate film is very thin, and thus

inertia forces are neglected, that is, gravity is the only body force considered.

5. The vapor is in a saturated state and the vapor-liquid interface is at the saturation temperature of the vapor.

6. The cooling surface temperature is everywhere constant.

Within the restrictions of the above assumptions Nusselt derived the following equation for a vapor condensing on a vertical surface of height L.

$$\bar{h} = 0.943 \left[\frac{\rho_l (\rho_l - \rho_v) h_{fg} k^3}{\mu_l L (T_{sv} - T_s)} \right]^{1/4} \qquad (7.1.1)$$

7.2 THEORY OF DROPWISE CONDENSATION.

Although dropwise condensation has been a known phenomenon for the past fifty years, it has not been subjected to the same degree of mathematical development as filmwise condensation. The major reasons have been twofold; first, the physical nature of the phenomenon is very complicated and the mechanism was not understood; second, since no one could develop a practical scheme for promoting dropwise condensation there has been little more than academic interest in it. However, it is known

(1) that when dropwise condensation occurs there is a marked increase in the rate of heat transfer to a surface.

For filmwise condensation, Nusselt needed only to consider a fully developed laminar film of condensate, where the only surface physics involved was the requirement that the condensate completely wet the cooling surface. The surface physics for dropwise condensation is far more complex, as will be shown in the following discussion. The phenomenon is presented from a microscopic kinetic theory point of view. The results of the experimental portions of this research is correlated with the equations developed in section 9.0.

7.3 SURFACE PHYSICS OF DROPWISE CONDENSATION.

An understanding of what takes place at microscopic levels when a vapor condenses in a dropwise fashion is of fundemental importance. In the following presentation the following questions will be discussed.

1. What is a vapor and a liquid?
2. How does a vapor condense on a surface?
3. What is the nature of the physical forces involved in the formation of dropwise condensation?
4. What is the most probable way a condensate droplet is formed at molecular levels?

5. How does a droplet grow once it is formed?

The above questions are answered by using arguments offered from the kinetic theories of matter. A basic assumption in kinetic theory is that the system being studied is in a state of complete equilibrium. This assumption will be modified for the case of vapor condensation where there exists a finite temperature difference between the vapor and the condenser surface. It is assumed that the system being studied is in a state of dynamic thermal equilibrium. The equation of state for a perfect gas will be used from time to time in this development.

The above limitations will be overlooked, and as a first order approximation the kinetic theory of gases and the perfect gas law will be assumed to give an approximate description of the behavior of a vapor. A brief study of the mathematics involved when intermolecular forces and finite molecular size are included, leads one to further justify the use of the more simple approach. In engineering science the utility of a result is more important than the exactness of the assumptions used to arrive at the result.

Any known real gas which is subjected to a pressure below its critical pressure is capable of being liquified. A look at a constant temperature line on a P-V coordinate

system when T is less than $T_{critical}$ shows that the curve is discontinuous at the saturated liquid line and again at the saturated vapor line. Thus, the nature of the condensing phenomenon does not allow the use of continuous mathematical equations of state to describe the complete transition from a gas to a liquid. Gases that obey van der Waals equation of state are exceptions to the above statement. A van der Waals gas is capable of certain metastable states, that from a theoretical point of view might allow a smooth transition from a gas to a liquid at pressures below the critical pressure. It should be noted, however, that such a transition has never been observed in the laboratory.

Throughout this discussion a vapor will be defined as a gas like substance that can be liquified with very small temperature reductions. At a given temperature, the pressure at which a vapor and liquid can co-exist in stable equilibrium is the saturation pressure.

The molecules of a liquid, as well as those of a vapor, are in a condition of continual motion. The open surface of a liquid creates the possibility that some molecules will penetrate the surface and enter the vapor above the liquid. Complete equilibrium is established when the number of molecules leaving the liquid surface to enter the vapor is exactly balanced by the number of

molecules returning from the vapor in a given time interval. The number of molecules leaving the liquid surface at a given temperature is proportioned to the area of the open surface. The number of molecules returning to the liquid surface is proportional to the open surface as well as the vapor pressure. Thus, the equilibrium pressure will depend only on the temperature of the liquid.

In the case of condensation on a liquid surface, the liquid surface is at a lower temperature than the saturated vapor. The net result is that the liquid captures and retains more molecules than it looses in a given time interval.

Since vapor molecules, on the average, possess more energy than those of the liquid, the condensation process must be accompanied by an evolution of energy. Energy released in this manner due to cohesion between molecules is called the latent heat of condensation. The latent heat of condensation will be assumed to be identical to the latent heat of evaporation.

So far the idea of molecular cohesion has been discussed without qualification. A short discussion of some of the more classic theories on the origin of cohesion in liquids is in order. The following discussion of intermolecular energies is summarized from material in refer-

ence (11).

W. H. Keesom (1912, 1922) explained cohesion as the interaction of permanent dipole moments, that is, moments created by the separation of positive and negative charges in the molecule. The relative magnitude of the interaction energy depends on the relative orientation of the dipoles. The phenomenon is called the orientation effect. The mean interaction potential energy between two dipolar molecules is given by,

$$U_o = -(2/3)(u^4/r^6 k T) \qquad (7.3.1)$$

where:

k= Boltzmann gas constant

u= dipole moment

r= distance between molecules

P. Debye (1920-21) showed that the moment induced by a dipolar molecule onto an adjacent molecule gives rise to an additional attractive energy called the induction effect, which is given by,

$$U_i = -(2 a u^2/r^6) \qquad (7.3.2)$$

where:

a= polarizability of the molecule

Because of certain phenomenon not explained by the considerations F. London (1930) derived the following

interaction energy equation from the theory of quantum mechanics.

$$U_d = -(3/4)(h_p V_o a^2/r^2) \qquad (7.3.3)$$

where:

h_p = the planck constant

V_o = characteristic frequency of the molecule.

The energy produced by this effect is called the dispersion effect. It is called the dispersion effect because the oscillations which produce the attractive force are also responsible for the dispersion of light by molecules. The dispersion effect applies to nondipolar as well as dipolar molecules. It is also additive for all pairs of molecules, and thus accounts for the phenonmenon of cohesion for molecules that do not have dipole moments.

A comparison of the relative magnitude of the interaction energies are listed below for hydrogen and water.

	DIPOLE MOMENT	ORIENTATION EFFECT	INDUCTION EFFECT	DISPERSION EFFECT
H_2O	1.8	190	10	47
H_2	0	0	0	11.3

The above discussion clearly points out the nature of the intermolecular forces that bind liquid water molecules together. For example, the forces act over very short molecular separation distances as is indicated

by the inverse relationship of high powers of r. The orientation effect is very large for water molecules and is also a function of the inverse of the temperature T. Thus, as the liquid temperature is lowered the forces of cohesion due to this effect get larger. This fact helps explain the higher capture rate of molecules, that is, the higher constant pressure heat flux when the degree of subcooling of a condenser surface is increased below the saturated vapor temperature T_{sv}.

It is not difficult to understand the high surface tension exhibited by water when one considers the cohesive forces discussed above.

A molecule in the interior of a liquid is completely surrounded by other molecules, and thus the resultant attractive force is zero. A molecule in a surface is subjected to a net resultant inwards attraction force. This is due to the fact that the liquid contains more molecules per unit volume than the vapor. A result of this inward pull causes the surface of a liquid to always contract to the smallest possible surface area. This is why drops of liquid assume a spherical shape, that is, the surface which is minimum for a given volume.

As a result of a liquids tendency to contract, a surface behaves as though it were in a state of tension, and it is possible to assign a definite value to this

surface tension, which is the same at every point and in all directions along the surface of the liquid. The surface tension is defined as the force acting at right angles to any line in the surface. Let us now consider the effects of surface tensions on a drop of water surrounded by water vapor and sitting on a solid surface.

The energy of adhesion between two surfaces was first formulated by Dupr'e(22) in 1869. For a three-component system composed of a non-wetting solid surface, a water droplet and water vapor, the Dupr'e relation would be written as follows:

$$W_{sl} = \sigma_{sv} + \sigma_{lv} - \sigma_{sl} \qquad (7.3.4)$$

Where W_{sl} is the energy required to remove the droplet from the solid surface and σ_{lv} is the surface tension between the liquid and its vapor, and σ_{sv} and σ_{sl} are the surface tensions between the solid and vapor or the liquid, respectively.

A relationship between the three surface tensions in equation 7.3.4 can best be illustrated by the introduction of the contact angle concept. The contact angle is defined as the angle formed at the adge of a droplet between the solid surface and a line which is tangent to the drop surface at that point. The contact angle is always measured outward from the inside of the drop. The

relationship between contact angle and the surface tension forces is illustrated in the following sketch.

For $\theta > 90°$, non wetting For $\theta < 90°$, wetting

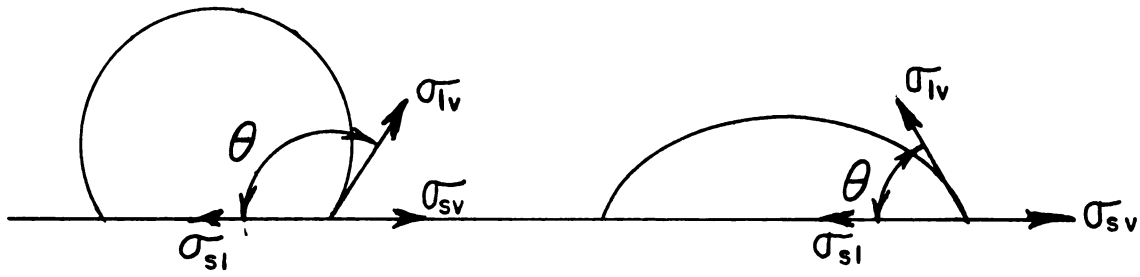

Addition of the vectors in the above diagram results in the following relationship,

$$\sigma_{sv} = \sigma_{sl} + \sigma_{lv} \cos\theta \qquad (7.3.5)$$

By combining equations 7.3.4 and 7.3.5 the equation developed by Young(22) is obtained.

$$W_{sl} = \sigma_{lv} (1 + \cos\theta) \qquad (7.3.6)$$

This equation is a more useful relation than equations 7.3.4 or 7.3.5 since σ_{sv} and σ_{sl} can't be measured easily or accurately.

Wetting of a solid surface implies that the contact angle is less than 90°. In general, surfaces with contact angles greater than 90° tend to be strong non-wetters. From equations 7.3.4 and 7.3.6 the cosine of the contact angle can be written as follows.

$$\text{Cos}\,\theta = \frac{\sigma_{sv} - \sigma_{sl}}{\sigma_{sv}} \qquad (7.3.7)$$

Thus, the following conditions can be stated for wetting and non-wetting,

Wetting $\sigma_{sv} - \sigma_{sl} > 0$ (7.3.8a)

Non-wetting $\sigma_{sv} - \sigma_{sl} < 0$ (7.3.8b)

As an example, water has a liquid-vapor surface tension of about 60 dynes/cm at 212°F. A water droplet in contact with its vapor and a horizontal teflon surface has a contact angle of about 115°.

The above discussion, thus, shows that the contact angle depends on the relative magnitude of the adhesional energy of the solid and liquid, and the cohesional energy of the liquid. Or, from a microscopic view point, the relative attraction between molecules of the solid and liquid and between the liquid molecules themselves.

It should be noted that a drop sitting on a vertical surface has a different contact angle at the top and bottom due to the distortion caused by the weight of the drop. Such variations in contact angle have the greatest effect on a drop that is heavy enough to roll down the

surface. It was noted in section 5.0 that this type of phenomenon becomes more important as the height of the condenser surface is increased.

7.4 SURFACE ADSORPTION PHENOMENON.

Adsorption is another surface phenomenon that may be important to dropwise condensation. Adsorption is the term used to describe the existence of a higher concentration of a vapor at the surface of a liquid or solid than is generally present in the bulk of the vapor. A solid or liquid surface possesses a residual force field. Adsorption results from the tendency of the free energy of a surface to decrease. Langmuir(12) showed that because of the rapid drop of intermolecular forces with distance the adsorbed layers are most likely no more than a single molecule in thickness. This view is presently accepted for adsorption at low pressures or at moderately high temperatures. However, at or near their saturation point the adsorbed molecules can hold other vapor molecules by means of van der Waals forces. Thus, it is possible to have an adsorption layer with a multimolecular thickness. Van der Waals adsorption is characterized by heats of adsorption that are the same order of magnitude as the heat of vaporization for a given substance. Water has all the characteristics to allow it to have a van der Waal type adsorption. However, much

depends on the type of water vapor-solid surface being considered. Another important feature of adsorbed films is that they establish an equilibrium with a solid surface very rapidly after a fluctuation in either temperature or pressure. This fact helps explain the rapid growth rate of liquid droplets since the condensing of adsorbed vapor films may help in the feeding process for a droplet. Once a film is cleared from the surface, it is instantaneously replaced. Thus, one might conclude that this feeding process is essentially a constant rate process. It is likely that the film feeding process is most important when the droplets of liquid are very small.

Umur and Griffith(13) report that from experimental observations, they were not able to measure a liquid film of water between drops greater than a monolayer of molecules in thickness. The steam was condensed onto a polished gold surface and the condensate films were measured by a reflected light optical system.

The existence or nonexistence of a liquid film on the condenser surface is an important consideration, as was noted above. It is concluded that an adsorbed film no thicker than a monomolecular layer exists between droplets while steam condenses on a teflon surface. It may be possible, however, for multimolecular adsorbed films to exist in capillary cavities, as will be noted in the

following discussion.

The existence of an adsorbed monolayer film or a condensed monolayer film may be important to the nucleation of a droplet. This is illustrated by considering the solid surface profile shown in figure 7.4.1.

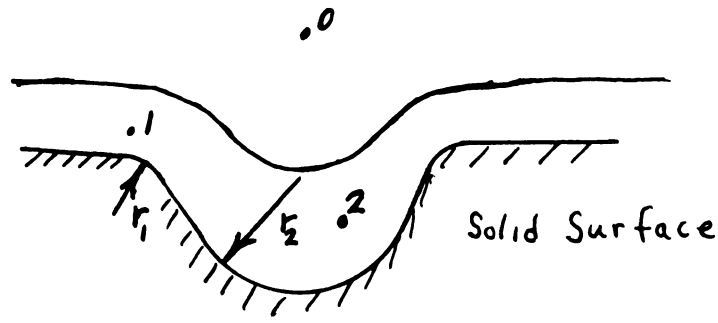

FIGURE 7.4.1 Adsorbed Vapor Film On A Capillary Pore In A Solid Surface.

It is a well known fact of capillary physics that the pressure on the convex side of a curved fluid surface is less than the pressure on a concave side of the surface. Consider the spherical shaped cavity of radius r_2 with a circular rim of radius r_1. Point 0 represents the condition of the vapor in the neighborhood of the cavity. Point 1 represents the condition of the adsorbed film on the rim of the cavity and point 2 represents the condition of the film in the bottom of the cavity. Since the film is curved at point 1 and 2 we conclude;

$$P_1 > P_0 \quad , \quad P_1 - P_0 = \frac{2\sigma_{lv}}{r_1} \qquad (7.4.1)$$

$$P_2 < P_0 \quad , \quad P_0 - P_2 = \frac{2\sigma_{lv}}{r_1} \qquad (7.4.2)$$

However $$P_0 = P_2 \qquad (7.4.3)$$

Thus, equations 7.4.1, 7.4.2 and 7.4.3 lead the conclusion that,

$$P_1 > P_2 \qquad (7.4.4)$$

and $$(P_1 - P_2) = 2\sigma_{lv}(1/r_1 + 1/r_2) \qquad (7.4.5)$$

Thus, the adsorbed film which acts like a membrane under tension trys to assume the smallest possible area per a given enclosed volume. Equation 7.4.4 leads to the conclusion that any molecules adsorbed at point 1 will flow to point 2 under the pressure differential (P_1-P_2) as given by equation 7.4.5. Note that for this development to be valid the adsorbed molecules in the film must be close enough to each other to be attracted by van der Waals forces of cohesion. It is significant to note that it is not necessary for the adsorbed film to cover the entire surface for the above arguments to be valid. The above discussion has not assumed any type of condensation. For example, the discussions would be true even if the solid surface was at or above the saturation temperature of the vapor. If the surface temperature is below the saturation temperature of the vapor, condensation would take place. We, thus, see that the most probable conden-

sation site is at the bottom of the cavity where the temperature is lowest and where there exists a more abundant supply of low energy molecules. This point will be discussed further in section 8.0.

7.5 ANALYSIS OF VAPOR MOLECULE CAPTURE BY A SURFACE.

In order to understand the vapor condensation process it is desirable to know the number of vapor molecules that strike the condenser surface per unit area and per unit time. If one was to observe a surface, the following types of molecular collisions would be observed,

1. Molecules strike the surface and are adsorbed, that is, adhere permanently (are condensed).
2. Molecules strike the surface and bounce off immediately.
3. Molecules strike the surface and adhere but as a result of thermal agitation some molecules evaporate and return to the vapor again.

The net result is that molecules are continually coming to and leaving the surface. If the surface and the vapor are at the same temperature, thermal equilibrium is established and the number of molecules entering and leaving are equal. However, if the surface is at a lower

temperature than the vapor the average number of molecules that are adsorbed exceeds the average number that evaporate. So, the latent heat released by the adsorption of molecules exceeds the latent heat absorbed by the evaporating molecules resulting in a net heat transfer to the surface. If $\bar{N}$ is the number of molecules striking the surface per unit area and per unit time, and if α is the fraction of the total number of molecules which strike the surface that are condensed, then $\alpha \bar{N}$ is the number of molecules that condense per unit area and time. Also, if F_m is the fraction of the total surface covered with adsorbed molecules at any instant, then $(1-F_m)$ is the fraction of the surface that is able to receive molecules, assuming that only a single layer of vapor molecules can form on the surface at any instant. Thus, the condensation rate is $(1-F_m) \alpha \bar{N}$ molecules per unit area of the total surface per unit time. The rate that molecules evaporate will be assumed proportional to the number of molecules on the surface, which is indicated by the fraction F_m. Evaporation can, thus, be represented by ϵF_m, where ϵ is a constant for a given vapor and surface. Thus, if T_{sv} is the temperature of the saturated vapor and T_s is the surface temperature, then at equilibrium,

$$(1-F_m)\alpha \bar{N} = \epsilon F_m \quad \text{when } T_s = T_{sv} \tag{7.5.1}$$

and $(1-F_m)\alpha \bar{N} > \epsilon F_m$ when $T_s < T_{sv}$ (7.5.2)

Equation 7.5.2, thus, establishes the condition for condensation on a clean solid surface. It is most likely that α and ϵ are not strong functions of the degree of surface subcooling $(T_{sv}-T_s)$. F_m will be a function of the type of surface on which the molecule is condensing and $(T_{sv}-T_s)$. For example, water vapor condensing on a liquid water surface, may give a value of F_m which would probably be smaller than when water vapor condenses on a teflon surface. However, if α and ϵ are assumed to be constant, variations could be assumed to be part of the F_m term. $\bar{N}$ is a function of the state of the vapor only, as will be shown below.

From the kinetic theory of gases (37), the total number of collisions per unit area and per unit time, by molecules of all velocities is given by the following expression.

$$N = 1/4 \int_0^\infty v \, dn_v \qquad (7.5.3)$$

where:

dn_v = number of molecules per unit volume with velocities between v and $v+dv$

v = velocity of a group of molecules

Using the Maxwell velocity distribution function, that is,

$$dn_v = 4\pi n \left(\frac{m}{2\pi kT}\right)^{3/2} e^{-\frac{mv^2}{2kT}} v^2 \, dv \qquad (7.5.4)$$

Putting equation 7.5.4 into equation 7.5.3 and integrating over all velocities from zero to infinity gives,

$$\bar{N} = n \left(\frac{kT}{2\pi m}\right)^{1/2} \qquad (7.5.5)$$

The mass of vapor $\dot{M}_v$ striking the condenser surface per unit area and per unit time is obtained by multiplying each side of equation 7.5.5 by m, the mass of a single molecule.

$$\dot{M}_v = m\bar{N} = \rho_v \left(\frac{RT_{sv}}{2\pi}\right)^{1/2} \qquad (7.5.6)$$

where: ρ_v = density of the vapor.

R = gas constant of the vapor.

T_{sv} = saturated vapor temperature.

Consider water vapor in contact with a surface under the following conditions.

$P_v = 14.7$ psia

$R = 85.6 \quad \frac{ft - lb_f}{lb_m \, ^\circ R}$

$T_{sv} = 212^\circ F = 672^\circ R$

$h_{fg} = 970 \frac{BTU}{lb_m}$

$\rho_v = 0.0363 \frac{lb_m}{ft^3}$

Using this data it is now possible to calculate the heat flux to a condenser surface if it is assumed that all the molecules striking the surface are condensed.

$$Q = \text{heat flux} = \dot{M}_v \; h_{fg} \qquad (7.5.7)$$

$$\dot{M}_v = 7.33 \times 10^4 \; \frac{lb_m}{Hr\ ft^2}$$

Thus $Q = 7.10 \times 10^7 \; \frac{BTU}{Hr\,ft^2}$

It is interesting to note that the above heat flux is several hundred times greater than any heat flux that has ever been observed. This example gives an idea of the huge energy potential that exist for a condensing vapor. The calculation also provides a way of determining the rate at which vapor molecules were condensed on the teflon condenser surface used in this program. From equation 7.5.2 and 7.5.6 the general expression for the heat flux can be written as,

$$Q = (1-F_m)\, \alpha\, \rho_v\, h_{fg} \left[\frac{R\, T_{sv}}{2}\right]^{1/2} \qquad (7.5.8)$$

The calculation derived from equation 7.5.7 clearly shows that the product of the first two terms on the right side of equation 7.5.8 must be quite small.

7.6 EFFECT OF CONDENSING CONDITIONS ON DROP FORMATION AND GROWTH.

It has already been demonstrated that there exists a pressure difference across a curved liquid layer. Here, however, it will be shown that the surface tension of a liquid drop causes the pressure inside the drop to exceed its external pressure. As a first consideration, assume that a hemspherical droplet on a solid surface is in equilibrium with its vapor. Also, assume that the contact angle made by the drop is 90°. The following sketch illustrates the drop geometry being analyzed.

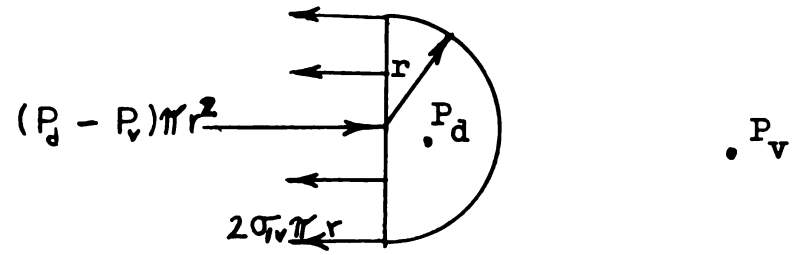

If P_d is the internal drop pressure and P_v is the external vapor pressure and σ_w is the surface tension, then for equilibrium the resulting forces must balance giving,

$$(P_d - P_v)\,\pi r^2 = 2\pi r\,\sigma_{lv} \qquad (7.6.1)$$

or

$$(P_d - P_v) = \frac{2\,\sigma_{lv}}{r} \qquad (7.6.2)$$

Thus, equation 7.6.2 shows that as the drop radius r grows small the pressure difference between the inside and outside gets large. Lord Kelvin proved from thermodynamic considerations that the vapor pressure is larger over a surface with large curvature. Thus, small droplets are less stable than larger ones. This fact is clearly shown in the following equation from reference (38).

$$\ln P_r/P_v = \frac{2 \sigma_{lv} v_f}{rRT} \qquad (7.6.3)$$

In the above equation P_r is the vapor pressure corresponding to the drop radius r. Under a given set of conditions equation 7.6.3 can be used to calculate the critical radius. Let T be considered the drop temperature which will be the same as the solid surface temperature T_s. P_v then is the saturated vapor pressure for a flat liquid surface corresponding to the drop temperature T_s. P_r is then interpreted as the vapor pressure of the vapor that is about to be condensed P_{sv}. With these conditions the critical drop radius can be written from equation 7.6.3 as,

$$r_c = \frac{2 \sigma_{lv} v_f}{RT_s \ln P_r/P_{vs}} \qquad (7.6.4)$$

A drop of radius r_c would be in equilibrium with its vapor at the pressure P_r. However, the vapor condensed

on the drop would represent a supersaturated condition, since $P_{vs} < P_r$. Thus, equilibrium would not be stable since evaporation of a few molecules would cause the drop radius to decrease. This would cause the drops vapor pressure P_r to increase and the drop would continue to evaporate. On the other hand, if a few molecules of vapor should condense, r would increase, P_r would decrease and the drop would continue to grow. In the case where a drop is sitting on a subcooled condenser surface it would continue to grow by this mechanism until the temperature of the outer most surface of the drop approaches the surrounding vapor temperature.

Consider saturated steam condensing at a pressure of 14.7 psia on a drop promoted condenser surface. Figure 7.6.1 shows the variation of r_c as a function of the temperature difference between the saturated steam vapor and the condenser surface. Very small changes in the condenser surface temperature between a value of $(T_{sv}-T_s)$ of 0°F and 2°F causes large variations in the magnitude of the critical drop radius. This helps explain why the dropwise condensation process slows down as $(T_{sv}-T_s)$ is decreased. Also, at $(T_{sv}-T_s) = 0$, $r_c = \infty$, thus, there can be no drops formed on the surface at this temperature and at most a monolayer of vapor molecules would exist on the condenser surface. It is reported in reference (28) that condensation requires $(T_{sv}-T_s)$ to be at least 0.05°F, for

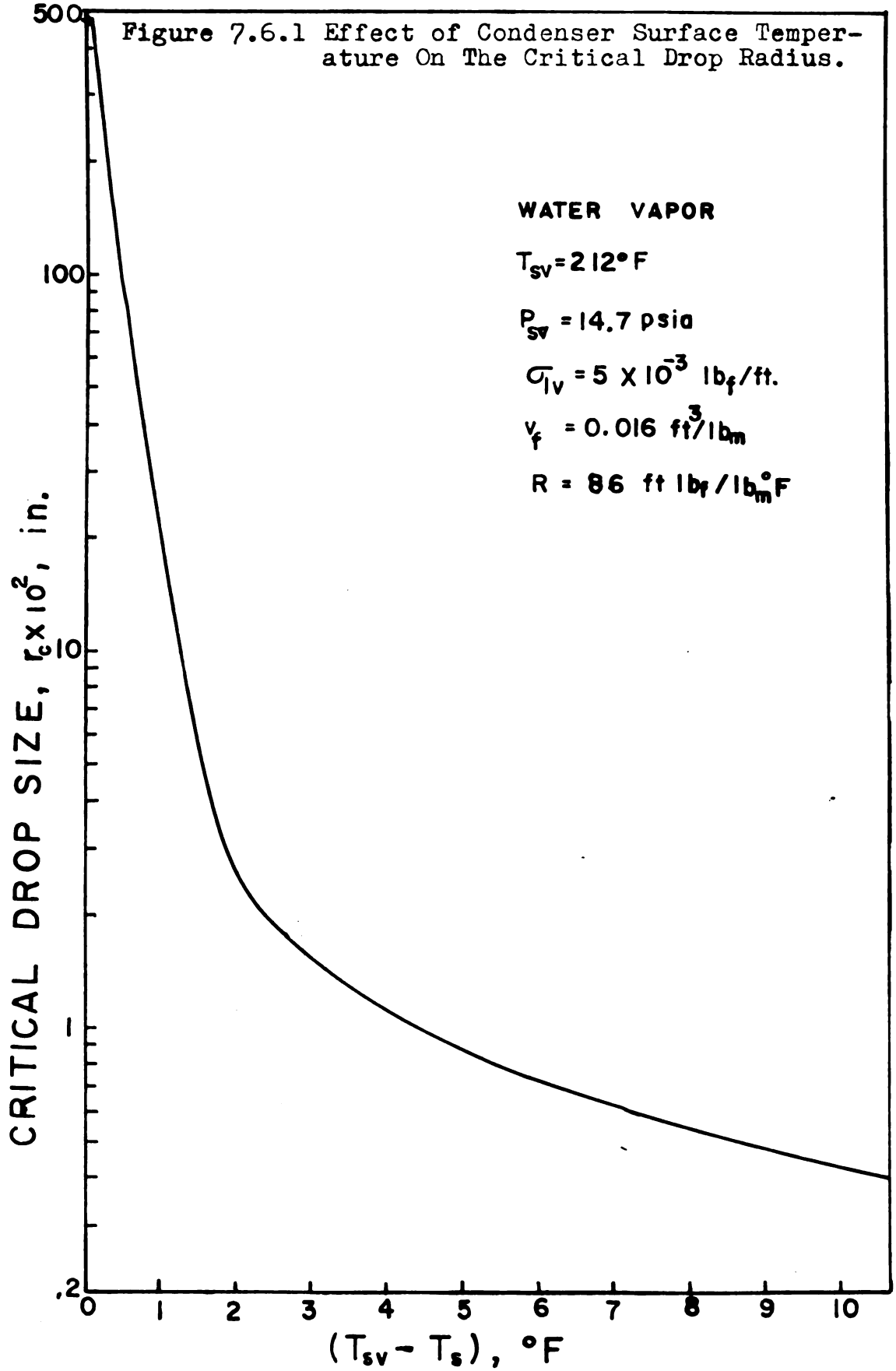

Figure 7.6.1 Effect of Condenser Surface Temperature On The Critical Drop Radius.

water vapor at atmospheric pressure, if a balance is to be maintained during the transport of vapor to a condenser surface. It should be noted, also, that at 0.05°F the critical radius of a stable drop would be quite large and an active nucleation may be impossible.

Figure 7.6.1 shows the r_c curve to flatten somewhat when $(T_{sv}-T_s)$ is greater than about 4°F. Extension of the curve to $(T_{sv}-T_s) = 180°F$, or $T_s = 32°F$, shows that the critical drop radius declines to a value of 2.2×10^{-4} microns, it can be seen that the combination of two water molecules would create a drop larger than the critical radius at $T_s = 32°F$. In contrast, at $(T_{sv}-T_s) = 0.1°F$, it would take 4.35×10^4 molecular diameters to equal the critical diameter of a stable drop.

It is concluded that dropwise condensation requires nonwetting (see equation 7.3.8b) as a necessary but not sufficient condition. As has been shown, surface roughness and surface temperature are also important considerations.

7.7 REVIEW OF PAST MECHANISM THEORIES.

There has been several attempts to explain the mechanism of dropwise condensation. Jakob(20), in 1936, was the first to suggest a theoretical model to describe dropwise condensation. This theory has been supported in re-

cent studies by Baer and McKelvey(21), as well as Westwater and Welch(3). Jakob's theory states that initially a surface condenses a thin layer of either steam or water which grows to a certain unstable critical thickness (about 0.001mm), and then fractures and rolls itself together to form drops. The high heat transfer rate is explained by the fact that the forming of drops leaves a portion of the surface bare. Fresh steam is then condensed very quickly on these bare spots to form a new film of condensate. The exact physical nature of the film was not proposed. It was only mentioned that the film layer may consist of steam or water or mist. The recent papers (3, 21), however, have considered the film to be water. Drop growth was proposed to be caused by capturing more film and other drops. It was assumed that the thickness at which the film would fracture to form drops is a function of the particular surface, but is independent of the cooling rate. The cooling rate only determines the time required for the film to reach its critical thickness.

As was mentioned in section 7.4, the existence of a surface film greater than a monomolecular layer in thickness is not probable. This conclusion was supported by a considerable body of theoretical as well as experimental evidence. We, thus, note that the existence of a monomolecular film 2.28×10^{-4} microns thick is possible but a film 1 or more microns thick is not likely.

The experiments of Umur(13) established that there was a film when steam was condensed on a chemically promoted copper surface, however, no film existed when a clean gold surface was used. In the case of teflon there is also no chemical promoter present, and it is unlikely that a surface film plays the part suggested by Jakob(20). The lack of a film of significant thickness was also concluded in a recent microscopic study of dropwise condensation on a horizontal surface made by McCormick and Baer(4).

In 1936, Eucken(28) postulated a model for dropwise condensation. According to his theory the first drops form around a nuclei of supersaturated condensed vapor molecules. In the close neighborhood of the droplets the monomolecular layer is not supersaturated, since supersaturation vanishes when condensation occurs. The density of the layer close to the droplets is smaller than at a distance. The drop grows through a surface diffusion process, caused by the density gradient, which draws the supersaturated vapor layer in through the edge of the droplet. He also assumed that direct condensation takes place near the edge of the droplet, since the drop surface temperature at this point is the same as the cooling surface. Eucken showed in his analysis that only about 0.4% of the impacting molecules are immediately reduced to the liquid state. According to Eucken's analysis, the distance that the surface concentration gradient is sufficiently large

may only be about 1 micron in width.

In 1939, Emmons(29) proposed a theory somewhat similar to Euckens. Like Eucken, Emmons assumes that the space between the drops is covered by a supersaturated layer of vapor molecules. He assumed that condensation is maintained by strong mechanical turbulence caused by the rapid decrease in pressure near the cooling surface as a result of condensation. These eddy currents are assumed strongest in the vicinity of the drops edge. Thus, Emmon's concept deviates from Eucken's theory by considering turbulent flow as the driving mechanism instead of surface diffusion. Emmons considered the following conditions as favorable to dropwise condensation.

1. Low rate of condensation.
2. Low condensate viscosity.
3. High values of the liquid to vapor surface tension and values of the contact angle greater than 90°.
4. Smoothness of the condenser surface.

Emmons also points out that the rate with which two drops merge after touching may be an important consideration. If, after touching, two drops merge so slowly that other drops are able to combine with them on all sides, the surface will be covered with a film formed by the merging drops. This effect may be caused by high rates of conden-

sation.

In 1949, Fatica and Katz(9) derived an equation for predicting the film coefficient for dropwise condensation. They explain the heat transfer in terms of heat conduction across drops. The condenser surface temperature is considered to be equal to the saturation temperature of the vapor both between and at the surface of drops. The surface area covered by drops is assumed to be at a lower temperature. The heat transfer resulting from this temperature distribution is averaged over a group of drops. Their mechanism assumes that the vapor condenses into a large number of uniform macroscopic drops that cover about 45% of the surface. The 45% factor was supported by Hampson(15) and by Welch(10). Drops are assumed to grow until a size is reached that will cause them to roll down an inclined surface sweeping it bare of condensate. The roll-off drop size is given as a function of the inclination of the surface, the difference between advancing and receding contact angles, the surface tension of the liquid and the liquid density. Other major assumptions are:

1. The drops are segments of spheres, all with the same contact angle.
2. The fraction of area covered by drops remains constant throughout the cycle.
3. The condensate is distributed uniformly over

the cooling surface.

4. The critical size is the same for all drops.

5. Non-condensable gases are not present.

The equation resulting from this analysis gives the condensing film coefficient h as a function of the overall coefficient U. Since U contains h, the equation is not explicit in terms of h.

Sugawara and Michiyoshi(27) derived an equation for dropwise condensation film coefficients using a model and assumptions which were essentially the same as those of Fatica and Katz. Sugawara extended Fatica's analysis to include the sweeping cycle as well as the adhering period. Sugawara claims that the average film coefficient is the same for both the adhering and sweeping period. Sugawara's equation has the same shortcomings as the one developed by fatica, that is, the film coefficient is expressed as a function of the overall heat transfer coefficient.

McCormick and Baer(4) in a recent study (1963) used a modified Fatica and Katz type analysis to develop an equation to predict dropwise condensing film coefficients. They propose that drops are nucleated at randomly arranged active sites. The density of these sites being dependent on surface roughness. Their heat transfer theory assumes that heat is transferred by conduction through very small

drops. They, also, conclude that the area between the small drop is not covered by a relatively thick liquid film through which heat is transferred.

It is interesting to note that in an earlier (1958) study Baer(21) concluded that heat is transferred mainly by conduction across a relatively thick liquid film in the region between the visible drops. This paper follows the lines of thinking proposed by Jakob(20).

A study published in 1965 by Umur and Griffith(13) was made to obtain information about conditions under which condensation can occur. Their major contribution was an experimental examination of condenser surfaces, using an optical method that was capable of detecting surface films of molecular dimensions. They concluded the following things:

1. The area between the drops does not have a liquid film greater than a monolayer of molecules in thickness.
2. No net condensation takes place on the area between drops. Hence, nearly all the energy transferred to the cooling surface is transferred through drops.
3. The most probable drop nucleation sites are wetted pits and grooves in the condenser surface.

4. The growth rate of small drops is significantly dependent on the vapor pressure.

The above reviews present the more important assumptions that have been applied to the mechanism of dropwise condensation. It can be seen that all the authors have contributed information. The efforts that were supported by experimental data made the greater contribution to the advancement of dropwise condensation technology. The past theories can be broken down into the following schools of thought.

1. The film fracture concept started by Jakob(20).
2. The drop nucleation concept started Eucken(28) as well as by Emmons(29).

The developing body of experimental and theoretical evidence indicates that the drop nucleation phenomenon is the most likely way for a vapor to condense on a surface which is not wetted by the condensate.

It is also quite evident that none of the theories proposed in the past answer all of the questions. For example, the study by Umur(13) indicates that wetted pits in the surface would be required to form dropwise condensation. If this were true it would not be possible to develop dropwise condensation on a teflon surface which has no wetted pits. However, perfect dropwise condensation was ob-

served on teflon during the present program. It is, thus, evident that this aspect of Umur's conclusions must be modified.

A comparison of the past mechanism theories, also shows that there are many areas of thought that overlap. The effort then is to abstract ideas from these past theories, combine these ideas with facts and ideas developed during this program, and then propose a new mechanism theory based on these conclusions.

Most of the previous investigations have only involved themselves with what happens for a single drop. The effort in this work will be to develop an equation for the condensing film coefficient h, which is based on the mechanism theory as well as the experimental data.

8.0 PROPOSED MECHANISM OF DROPWISE CONDENSATION.

The mechanism of dropwise condensation is a very complicated phenomenon. The complicated nature of this process makes it most difficult to apply mathematical and physical laws to the entire sequence of events that are involved during dropwise condensation of a vapor. It is possible to investigate specitic events in the process and in so doing develop an intuition about the various parameters that are involved. It is the purpose of this section to look into the process and try to define and describe what takes place.

In the past, the primary effort has been to describe how a single drop is formed and how it grows. Such a limited objective, although worthwhile, does not lead to mathematical expressions that can be used to make design calculations for heat transfer problems. In general, the transfer of heat to a surface is an overall averaging process. Thus, one would want to search for a general expression based on physical principle and confirmed by experimental data. This point will be pursued in section 9.0.

If one has established that a condensate will not wet a surface the next thing to consider is the physical nature of the surface itself. It has been observed that roughness on a macroscopic scale favors filmwise conden-

sation. It will be shown that roughness on a microscopic scale favors dropwise condensation. When one speaks of roughness, there must be a qualification of the relative magnitude involved. Consider the following types of surfaces.

1. Completely smooth and free of any type of imperfection.
2. Smooth from a macroscopic point of view but having small cavities a few microns in diameter when considered from a microscopic point of view.

The macroscopicly rough surface will not be discussed for reasons mentioned above.

A type 1 surface nucleates drops in a completely random fashion. That is, the drops do not originate in or on any specific section or spot on the condenser surface with respect to time. This type of condensation represents the more general case to be presented for dropwise condensation. It is proposed that the drop nucleates at a given spot and then grows from that point.

There is a considerable body of evidence that drops nucleate in a supersaturated vapor. This evidence is very well summarized in a paper by Hill, Witting and Demetri (32). They were concerned with condensation of vapor during rapid expansion of a vapor through a nozzle. Although

the probelm is different, the condensation is quite similar to the condensation on a cool solid surface. In the case being studied, supersaturation is caused by the vapor coming into contact with the cooler surface. The greatest degree of supersaturation would occur at the surface itself. Thus, it is reasonable to assume that drop nuclei will form on the condenser surface only.

The criterian for a stable drop and for drop growth was presented in section 7.6, equation 7.6.4 (also see figure 7.6.1). It was shown that if a drop achieved a radius greater than the critical radius r_c, the drop would continue to grow. It is not difficult to see that if a drop is nucleated away from the condenser surface the supersaturation vanishes upon condensation and the drop evaporates. This explains why one never sees a fog or mist surrounding a condenser surface. This also supports the conclusion that only nucleation on the condenser surface needs to be considered.

In order to determine the number of nucleations on a smooth type 1 condenser surface per unit time and per unit area, consider the following analysis. The potential energy difference between n liquid molecules in an n-sized drop, and n molecules in the vapor phase is,

$$\Delta E = h^*_{fg} n - 2\pi r_n^2 \sigma \qquad (8.1)$$

where: r_n = hemispherical drop radius.

h^*_{fg} = heat of vaporization per molecule.

σ = surface tension between the liquid and vapor.

$$r_n = \left(\frac{3\,n\,m}{4\pi\rho_f}\right)^{1/3} \tag{8.2}$$

Using equation 8.2; equation 8.1 becomes,

$$\Delta E = h^*_{fg} n - \lambda n^{2/3} \tag{8.3}$$

where:

$$\lambda = \left[\frac{3\pi m}{\rho_f}\sqrt{\frac{\sigma^3}{2}}\right]^{2/3} \tag{8.4}$$

The function ΔE has a maximum which can be used to define the number of molecules in a drop of critical size r_c.

$$\frac{d(\Delta E)}{dn} = 0 \tag{8.5}$$

Thus equation 8.5 gives,

$$n_c = \left(\frac{2}{3h_{fg}}\right)^3\left(\frac{3\pi m}{\rho_f}\right)^2\left(\frac{\sigma^3}{2}\right) \tag{8.6}$$

Drops containing n_c molecules can be considered as condensation nuclei. A drop of the n_c size will continue to grow if its size increases to (n_c+1) molecules since the total energy of the system decreases. Note, also, that a (n_c-1) drop would shrink or evaporate for the same reason.

Under equilibrium conditions it is reasonable to assume The Maxwillian type size distribution function given by equation 8.7. Thus, the number of n sized drops f(n) can be written as,

$$f(n) = \frac{N_s}{n_c} \quad \exp -\left(\frac{h_s^* n - \lambda n^{2/3}}{n_c k T_{sv}}\right) \qquad (8.7)$$

Where N_s is the number of molecules in an adsorbed monolayer per unit surface area.

The distribution given by equation 8.7 is unstable since both (n_c+1) and (n_c-1) drops grow or shrink with a resulting decrease in the total energy.

The formation of a nucleation sized n_c drop does not insure that it will grow. For growth a (n_c+1) drop would be required. Thus, to get an accurate estimate of the number of nucleation sites formed per unit time and area, the transfer from n_c drops to (n_c+1) drops must be considered. By considering a distribution function D(n,t), that is a function of both time and drop size, it is possible to write the following transfer function equation.

$$J(n,t) = \alpha(1-F_m)\bar{N}A_n D(n,t) - \epsilon L(n+1)A_{n+1} D(n+1,t) \qquad (8.8)$$

where:

$(1-F_m)$=fraction of surface active to nucleation.

Under equilibrium conditions, in the absence of
measure the maximum rate of dissolution (reaction
given by equation 2.1. Using the Arrhenius
mode $f(\sigma)$ can be written as,

$$f(\sigma) = \frac{k_r}{D_r} \exp\left(\frac{\sigma^2 \Omega - \gamma \Omega^2}{kT}\right) \qquad (2.2)$$

Where k_r is the product of reaction
layer per unit surface area.

The dissolution D_r can be expressed in terms of the modified
edge beam $(\sigma_{ij}-p)$ and $(\sigma_{ij}-p)$ is zero
resulting dimensions in the bond zone.

The formation of a cavity (void) by the coalescence
not impede itself in will grow. The growth of $(\sigma_{ij}-p)$ zone
would be necessary. Thus, the rate of expansion is limited
the number of dislocations which intersect a unit length
area, the dislocation flow D_r should be $D_r(\sigma_{ij}-p)$ zone must be
considered. In considering a dislocation function
$D(x,t)$, such as a function of both time and deep time, it
is possible to write the following integral function
equation.

$$\dot{\varepsilon}(x,t) = \alpha(1-F_D)\rho_m b[\sigma_{ij}-p(x,t)] \qquad (2.3)$$

where:

$(1-F_D)$=fraction of available dislocations

A_n=surface area of an n sized drop

$\bar{N}$=number of vapor molecules striking the drop (see equation 7.5.5).

L(n+1)=The rate molecules evaporate from the surface of an (n+1) sized drop.

α =accomodation coefficient.

ϵ =evaporation coefficient.

Equation 8.8 is only concerned with the n drops that are capturing molecules and the (n+1) drops that are loosing molecules. The drops with these two classifications will be separated and analyzed as though drops of all other sizes do not exist. This is reasonable when $n=n_c$ since an (n_c-1) drop has a large probability of completely evaporating and an (n_c+1) drop is well on its way to a condition of very rapid growth. The (n_c+1) drop is also no longer in a state of equilibrium, however, the loss of one molecule puts it back into the equilibrium state. Under equilibrium conditions D(n,t)=f(n), and

$$J(n,t)=0 \tag{8.9}$$

and assuming that $\alpha = \epsilon$

$$L(n+1)\,A_{n+1} = \frac{(1-F_m)\,A_n\,f(n)}{f(n+1)} \tag{8.10}$$

At or near drop sizes $n=n_c$, the drops can be assumed to be in a state of quasi-equilibrium, which allows the

transfer function to be written as,

$$J(n,t) = (1-F_m)\bar{N}A_n f(n)\left[\frac{D(n,t)}{f(n)} - \frac{D(n+1,t)}{f(n+1)}\right] \qquad (8.11)$$

Equation 8.11 is similar to a derivative formula, and it will be approximated by,

$$J(n,t) = \alpha(1-F_m)\bar{N}A_n f\frac{d}{dn}\left(\frac{D}{f}\right) \qquad (8.12)$$

The following limits will be used on equation 8.12.

$$\lim_{n \to n_c}\left(\frac{D}{f}\right) = 1$$

$$\lim_{n \to n_{c+1}}\left(\frac{D}{f}\right) = 0 \qquad (8.13)$$

While quasi-equilibrium exists it is assumed that J is independent of both time and particle size, which gives the transfer equation as,

$$J\int_{n_c}^{n_c+1}\frac{dn}{A_n f} = -\alpha(1-F_m)\bar{N}\int_{n_c}^{n_c+1} d\left(\frac{D}{f}\right) \qquad (8.14)$$

Since near $n=n_c$ the drop size is not changing rapidly, it is reasonable to assume $A_n = A_{nc}$ and, thus treat it as being independent of drop size. The transfer function giving the nucleation rate is thus,

$$J = \frac{\alpha(1-F_m)\,\bar{N}\,A_{nc}N_s}{n_c\int_{n_c}^{n_c+1}\exp\frac{\Delta E}{n_c k T}\,dn} \tag{8.15}$$

Integration of equation 8.15 is accomplished by first expanding ΔE into a three term Taylor series about the point $n=n_c$.

$$\Delta E = \Delta E_c + 1/2\left(\frac{\partial^2 \Delta E}{\partial n^2}\right)_{n=n_c}(n-n_c)^2 \tag{8.16}$$

Thus,

$$\Delta E = \Delta E_c - 1/9\,\bar{n}_c^{\frac{-4}{3}}(n-n_c)^2 \tag{8.17}$$

As a first order approximation the second term on the right side of equation 8.17 will be neglected since n is restricted to the range n_c to n_c+1. With this simplification the nucleation rate equation can be written as,

$$J=\frac{\alpha(1-F_m)\bar{N}\,A_{nc}}{n_c}\exp-\left(\frac{h^*_{fg}\,n_c-2\pi\,r_c^2\sigma)}{n_c k T_{sv}}\right) \tag{8.18}$$

Using equation 7.5.6 and $A_{nc}=2\pi r_c^2$, it is possible to write equation 8.18 as,

$$J = \frac{3\alpha(1-F_m)N}{2\rho_f r_c}\left(\frac{R\,T_{sv}}{2\pi}\right)^{1/2} \exp - \left(\frac{h_{fg}}{RT} - \frac{3\sigma}{2\rho_f r_c RT}\right) \qquad (8.19)$$

The critical drop radius r_c is best estimated by using equation 7.6.4. Equation 8.19 should give a good estimate of the drop nucleation rate when the condenser surface temperature T_s is very near to the saturation temperature T_{sv} of the vapor. This is because equation 8.19 was derived for conditions approaching equilibrium. For example, when $(T_{sv}-T_s) = 0.1°F$ the nucleation rate is given by equation 8.19 as 1.7×10^{10} nuclei per square inch per second.

It is concluded that dropwise condensation will occur on a surface not wetted by the condensate when the surface is completely smooth and free of any type of preferred nucleation site. Further, the nucleation takes place on the surface between drops at random locations which change with time. Equations 8.19 shows that the nucleation rate on a type 1 surface is more than large enough to maintain the heat flux data derived from dropwise condensation experiments. The numerical values for α, and $(1-F_m)$ are discussed in section 9.0.

Since no real surface is free of microscopic grooves, pits and other physical imperfections, the type 2 surface

presents an actual surface that would occur during condensation. Microscopic pits and grooves, as well as small wetted spots provide preferred condensation sites. A preferred condensation site always remains fixed on the surface with respect to both time and location. Nucleation occurs more easily at a preferred site than at the random sites discussed above. This is why drops are observed to form a growth pattern on a condenser surface. Repeated drop growth at the same point was observed from the photographic studies made during this program. Preferred nucleation is also reported in a study by McCormick and Baer(4). McCormick and Baer concluded that nucleation takes place at randomly located preferred nucleation sites which remain fixed with respect to time. This conclusion was drawn from their observations of drop growth on a horizontal surface which was observed through a microscope. They report that repeated drop growth at surface scratches was most evident.

There were two types of preferred nucleation sites observed during this program. The largest type was formed by small holes or cracks in the teflon film. These cracks penetrated to the bare metalic surface. For metals like copper and aluminum these cracks were filled to the outer surface with metalic oxide. With stainless steel the cracks remained empty. In this type of site the condensate wets the bottom of the cavity. Inspection of the

teflon coated condenser surfaces through a microscope at 400X showed that the average wetted-preferred nucleation site is 0.001 inches in diameter and there are about 3×10^3 sites per square inch. The occurrence of this type of site would be less frequent when the teflon film is thicker and more frequent when the teflon film is thinner than the one used during this program.

The second type of preferred nucleation site is formed by small holes or cavities in the teflon surface that do not penetrate to the metal on which the teflon is coated. An inspection of the teflon film used in this program showed that there were a large number of these cavities present. Microscopic observations at 400X magnification showed that there were about 2×10^6 cavities per square inch. Each cavity was round with a diameter between 5×10^{-5} inches and 1×10^{-4} inches. The cavities appeared to be concave hemispheres. An analysis by McCormick and Baer(33) indicated that about 7.5×10^6 sites per square inch would be present. Tamman and Boehme (34) report that water vapor condensed from saturated air onto a horizontal condenser gave between 10^6-10^7 drops per square inch. They report that the number of observed drops depended upon the type of condenser surface metal used. A later report by McCormick and Baer(4) indicates that the number of nucleation sites was counted, and found to be about 5.6×10^5 nuclei per square inch. The data

reported in the above literature was taken for condensation at very small values of (T_{sv}-T_s) with a T_{sv} of about 70°F. It is quite likely that the nucleation sites reported are of the nonwetted-preferred type.

The nonwetted-preferred condensation site occurs for the following reasons.

1. The bottom of a cavity is at a lower temperature than its rim or the area between the cavities. This causes a vapor molecule to have a greater probability of condensing at the bottom of the cavity than anywhere else.
2. The number of times a single vapor molecule would collide with the walls of a microscopic cavity would be greater than for a flat surface. Since each collision decreases the molecules energy there will be more low energy condensible molecules in the cavity than elsewhere.
3. The curvature of the cavity causes adsorbed molecules to flow to the bottom of the cavity. The theory for this phenomenon was presented in section 7.4, also see figure 7.4.1.

The nonwetted-preferred condensation site is an important feature of all type 2 surfaces. It is evident that during actual condensation, both random and nonwetted-

preferred nucleation sites would occur at the same time. This conclusion explains the basic nature of dropwise condensation as it has been observed in the past as well as in this research.

The wetted-preferred condensation site can be neglected or assumed to be the same as a nonwetted-preferred site. It is important to note that a wetted-preferred site is not required for condensation to occur.

Nucleation at a preferred site is complete when the cavity is filled with condensate. Condensate will remain in the cavity even after a large drop vacates the area above the site. This means that the preferred site will cause a newly growing drop to grow faster and from a larger starting diameter than a randomly nucleated drop in the area between preferred sites. The preferred site is larger and more firmly anchored to the surface and would act as a collection point when coalescences start. Thus, a preferred site is an important factor in the growth mechanism.

At very low condensation rates, $(T_{sv}-T_s) < 0.1°F$, the critical diameter of a drop is the same order of magnitude as the preferred site diameter. Under this condition random nucleation would be very low and the preferred sites would account for almost all drops observed before coalescence takes place.

After nucleation the drops grow by capturing vapor molecules at their surface. It is also possible that the growth is supplemented by the flow of adsorbed molecules to the edge of the drop due to capillary forces. It seems reasonable that the direct bombardment of the drop surface by vapor molecules is the primary driving mechanism for drop growth, with the flow input from the surrounding monolayer of molecules being much less significant. Monolayer flow most likely plays a more important role in the nucleation phase of the condensation mechanism.

Once the first set of drops start coalescing the drop field changes from a group of one uniform size to another group of a larger uniform size. This first set of drops formed by coalescence will be located at preferred condensation sites. The combination of a number of small drops into a single large drop leaves a fraction of the surface clean of all but a monolayer of molecules. The nucleation and growth process then starts over again on these clean areas between the larger drops. The larger drops continue to grow primarily by capturing the newly created drops, and to a lesser extent by capturing vapor molecules. The larger drop field grows in this manner until there is a second major set of large drop coalescences into an even larger drop field, again leaving the surface clean between the newly formed drops. The second coalescence gives what will be defined as a third stage drop, the first coales-

cence a second stage drop, and nucleation a first stage drop. The third stage drop grows by capturing both first and second stage drops that grow nearby. This process continues until the drops are too heavy to stay in place on the vertical condenser surface. The drop then breaks loose and rolls to the bottom of the condenser surface leaving a vertical strip that is approximately the width of the maximum sized drop that started the roll-off process. The roll-off strip is completely cleared of drops allowing the entire process to start over in the strip path behind the roll-off drop.

The following things are postulated from the above discussion.

1. All the heat is transferred through first stage drops.
2. First stage drops occur only on the active fraction of the condenser surface $(1-F_m)$.
3. First stage drops are small enough so that the temperature gradient through them is not important. That is, the first stage drops are at the temperature of the condenser surface T_s.
4. First stage drops nucleate and grow from specific points. These points, or condensation sites, occur at preferred nucleation

points as well as random nucleation points. Most condenser surfaces have between 10^6 and 10^7 preferred nucleation sites per square inch. Random nucleation sites occur in the active areas at the rate of about 10^{10} sites per second per square inch.

5. Preferred nucleation sites determine the location of the second stage drops formed by the first sequence of coalescence.
6. 2^{nd}, 3^{rd}, -----, n^{th} stage drops do not contribute significantly to the transfer of heat, but rather, serve as condensate storage reservoirs. n^{th} stage drops grow by coalescing with drops of all sizes smaller than themselves.
7. Coalescence of drops and roll-off of maximum sized drops provides the mechanism for creating active heat transfer area on the condenser surface.
8. The area between the drops does not have a liquid film that is more than one molecular layer in thickness.

From the above proposed theory for the mechanism of dropwise condensation it is evident that the heat transfer to a surface is controlled by molecular phenomenon. Since

the heat is proposed to be transferred through microscopic drops that are at a constant temperature T_s, it is likely that the process is only weakly effected by the thermal conductivity of the condensate. Most known liquids that are capable of forming dropwise condensation (water, mercury, ethyleneglycol, etc.) have viscosities that are the same order of magnitude. It is possible that dropwise condensation phenomenon is not a strong function of viscosity, once it is established that the condensate does not wet the surface. Viscosity would have its greatest effect during drop coalescence, and drop roll-off. Liquid surface tension assumes the role in dropwise condensation that liquid viscosity plays during filmwise condensation.

Experimental data indicates that the dropwise condensation heat transfer coefficient is not a function of condenser surface height. The experimental evidence for this statement is discussed in section 3.0. The reason that condenser surface height or condenser geometry (a horizontal tube for example) does not effect the heat transfer coefficient can be seen from the fact that the entire process starts as a bare surface and ends up as maximum sized roll-off drops. The exact same process takes place at the bottom of the condenser surface as that which occurs in the middle or top of the condenser surface. Thus, it makes no difference from a theoretical point of view whether the surface is one inch or one foot tall, the average heat transfer rate will be the same.

9.0 MATHEMATICAL CORRELATION OF THEORY AND EXPERIMENTAL DATA.

The mechanism theory presented in the previous section is used in combination with a kinetic theory approach to yield heat transfer expressions for dropwise condensation. These expressions are then correlated to the experimental data. These expressions can be used to estimate the relative importance of the controlling parameters for dropwise condensation. They are also useful as heat transfer design equations. The general approach can be applied to dropwise condensation of any vapor, however, the various constants would have to be known for each substance. The final equations are specifically developed for water vapor and are not recommended for other fluids.

It was shown in section 7.5 that the mass of vapor molecules striking a unit surface area of a drop per unit time is,

$$\dot{M}_v = P_v\left(\frac{1}{2\pi R T_{sv}}\right)^{1/2} \qquad (9.1)$$

As was noted, a fraction α of these condense and the others are reflected. If it is assumed that the kinetic energy of the reflected particles corresponds to the drop temperature, the following becomes evident. For a drop on a surface, the mass flux from the drop is the same as the mass flux to the drop if it were surrounded by an environment at a pressure P_{vs} and a temperature T_s. This is

the same as considering equilibrium at T_s, P_{vs}, when the mass flux to and from a drop are equal. Thus, it can be concluded that the drop gains mass as though it has an influx at P_{sv}, T_{sv}, and it looses mass at conditions corresponding to P_{vs}, T_s. The rate of change of mass in the drop is thus given by the following mass balance.

$$\frac{dM_d}{dt} = 2\pi r^2 \alpha \left[\frac{P_{sv}}{\sqrt{2\pi R T_{sv}}} - \frac{P_{vs}}{\sqrt{2\pi R T_s}} \right] \tag{9.2}$$

The accomodation factor α is assumed not to be a function of temperature in equation 9.2. Note also that the drop is assumed to be at a uniform temperature T_s throughout.

If the drops are considered as hemispheres, the mass of drop M_d is,

$$M_d = \rho_f (2/3 \pi r^3) \tag{9.3}$$

The change in mass with respect to time due to the influx of vapor molecules is,

$$\frac{dM_d}{dt} = 2\pi \rho_f r^2 \frac{dr}{dt} \tag{9.4}$$

Equations 9.4 and 9.2 give the growth rate of a drop as,

$$\frac{dr}{dt} = \frac{\alpha}{\rho_f} \left[\frac{P_{sv}}{\sqrt{2\pi R T_{sv}}} - \frac{P_{vs}}{\sqrt{2\pi R T_s}} \right] \tag{9.5}$$

The heat flux due to the condensation of vapor on the drop is,

$$Q = \frac{h_{fg}}{2\pi r^2} \frac{dM_d}{dt} \tag{9.6}$$

Putting equation 9.2 into 9.6 gives,

$$Q = \alpha h_{fg}\left[\frac{P_{sv}}{\sqrt{2\pi R T_{sv}}} - \frac{P_{vs}}{\sqrt{2\pi R T_s}}\right] \tag{9.7}$$

Using the Causius-Clapeyron equation it is possible to get a relationship between P_{vs} and P_{sv}.

$$P_{vs} = P_{sv} \exp\left[-\frac{h_{fg}}{RT_s}\left(1 - \frac{T_s}{T_{sv}}\right)\right] \tag{9.8}$$

Putting equation 9.8 into 9.7 gives,

$$Q = \alpha h_{fg} \rho_v \left(\frac{gRT_{sv}}{2}\right)^{1/2}\left[1-\left(\frac{T_{sv}}{T_s}\right)^{1/2}\exp-\frac{h_{fg}}{RT_s}\left(1-\frac{T_s}{T_{sv}}\right)\right] \tag{9.9}$$

In section 7.5 it was shown that,

$$Q = (1-F_m)\alpha h_{fg} \rho_v \left[\frac{RT_{sv}}{2}\right]^{1/2} \tag{9.10}$$

A comparison of equations 9.10 and 9.9 shows that the fraction of active condensing surface $(1-F_m)$ can be written as,

$$(1-F_m) = \left[1-\left(\frac{T_{sv}}{T_s}\right)^{1/4}\exp-\frac{h_{fg}}{RT_s}\left(1-\frac{T_s}{T_{sv}}\right)\right] \tag{9.11}$$

It is possible to simplify equation 9.11 by observing that $(T_{sv}/T_s)^{1/2}$ will always be a number close to unity. Also, since the absolute value of the exponent of the exponential term is a number smaller than one, it is possible to make the following approximation,

$$1 - e^{-x} = x - \frac{x^2}{2!} + \frac{x^3}{3!} - \cdots \simeq x \quad , \quad x \ll 1.0$$

Using the above approximation equation 9.11 becomes,

$$(1-F_m) = \left[\frac{h_{fg}}{RT_s}\left(1-\frac{T_s}{T_{sv}}\right) \right] \tag{9.12}$$

The equation for the heat flux can now be written from equation 9.10 as,

$$Q=\alpha h_{fg}\left(\frac{g_o RT_{sv}}{2\pi}\right)^{1/2}\left[\frac{h_{fg}}{RT_s}\left(1-\frac{T_s}{T_{sv}}\right)\right] \tag{9.13}$$

Equation 9.13 gives a reasonable correlation for the data obtained during this program. Figure 3.1 shows the curve given by equation 9.13 and its relationship to the experimental data. Figure 9.1 shows that the slope of the heat flux curve given by equation 9.13 is too large. The slope is corrected to give a better correlation with the experimental data. The dimensionless correction factor is,

$$\frac{C}{(T_{sv}-T_s)^{4/3}} \tag{9.14}$$

where: $C = 1\ {}^{\circ}R^{4/3}$

Using this correction the heat flux equation 9.13 becomes,

$$Q = \left(\frac{\alpha C\, h_{fg}^2 \rho_v}{RT_s}\right)\left[\frac{g_o\, R}{2\pi T_{sv}(T_{sv}-T_s)^{2/3}}\right]^{1/2} \qquad (9.15)$$

The corrected heat flux curve given by equation 9.15 is also shown in figure 9.1.

The accomodation coefficient used in this study was 0.011. The exact value of α and any possible variation it may have with temperature is not known. Eucken(25) suggests that α may be about 0.004 for saturated steam at atmospheric pressure. This is supported by Alty and Nicoll(23) who showed from the results of evaporation experiments that $\alpha = 0.015$ at 12°C. This value was shown to decrease by 0.0001 for each 1°C of temperature increase. At 100°C α would be about 0.006 from these results. The value of 0.011 used in this program is within the range of values reported in the literature and is considered to be reasonable.

Calculations show that the heat flux as given by equation 9.15 is not strongly effected by small changes in α, over a wide range of $(T_{sv}-T_s)$.

An expression can now be written for the average heat transfer coefficient, defined by,

$$\bar{h} = \frac{Q}{(T_{sv}-T_s)} \qquad (9.18)$$

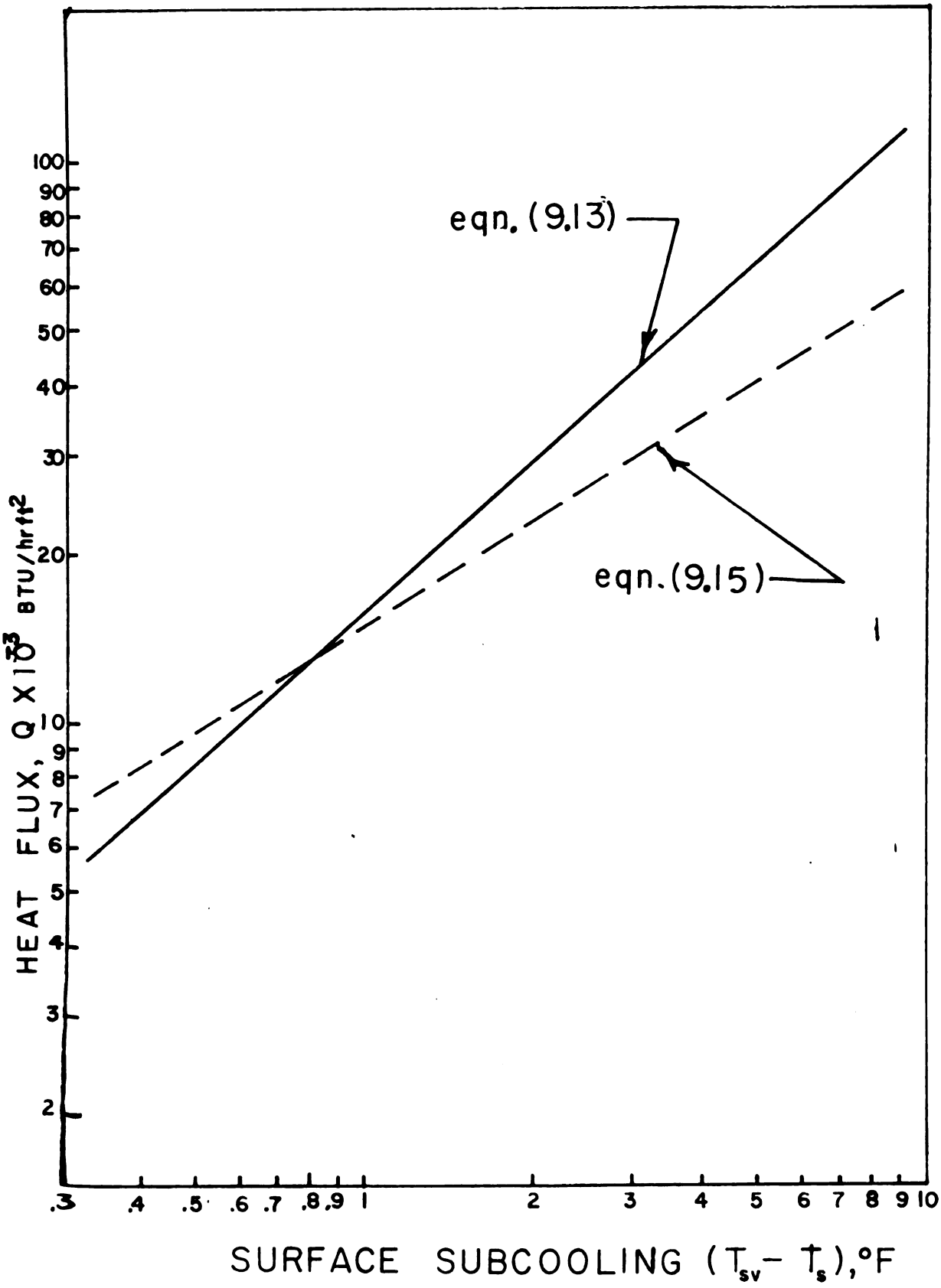

Figure 9.1 Heat Flux Theory Correction Curve.

Using the heat flux given by equation 9.15 equation 9.16 becomes,

$$\bar{h} = \alpha C \left[\frac{h_{fg}^2 \rho_v}{RT_s(T_{sv}-T_s)^{4/3}}\right] \left(\frac{g_o R}{2\pi T_{sv}}\right)^{1/2} \qquad (9.17)$$

Putting the constants into equation 9.17 gives the general expression for the dropwise condensation heat transfer coefficient for saturated water vapor.

$$\bar{h} = 816 \left[\frac{\rho_v h_{fg}^2}{T_s T_{sv}^{1/2}(T_{sv}-T_s)^{4/3}}\right] \qquad (9.18)$$

The dimensionless average Nusselt number is,

$$\overline{Nu} = \frac{\bar{h}L}{k_l} = 816 \left[\frac{\rho_v h_{fg}^2 L}{k_l T_s T_{sv}^{1/2}(T_{sv}-T_s)^{4/3}}\right] \qquad (9.19)$$

Where L is the height of the vertical condenser surface. Equation 9.18 is compared with experimental data in figure 3.2. Equation 9.18 is shown to give an excellent representation of experimental data over a wide range of $(T_{sv}-T_s)$.

Equation 9.18 contains no terms involving either the thermal conductivity of the condensate, condensate viscosity, or condenser surface height. The absence of the thermal conductivity is a result of the fact that the majority of the heat is assumed to be released in very small drops which do not offer significant thermal resistance

to the flow of heat. Viscosity will have the effect of slowing the drop growth rate by causing the coalescing time to be longer for fluids with high viscosity. We, thus, note that low viscosity favors dropwise condensation. Experimental data indicates that dropwise condensation is not strongly effected by condenser surface geometry. This conclusion is supported by the data presented in figure 3.2, where data from this program as well as data from other efforts are plotted together. Although the data from the various programs were taken from vertical surfaces of different heights as well as horizontal ½ inch O.D. tubes, the agreement with equation 9.18 is very good.

The effect of the above mentioned physical parameters on the dropwise condensation heat transfer coefficient should be the subject of future research.

It is concluded that equation 9.18 provides an adequate relationship for computing dropwise condensation heat transfer coefficients for saturated water vapor.

10.0 CONCLUSIONS

1. Dropwise condensation is not effected by condenser surface geometry.
2. The heat transfer coefficient and the heat flux are not independent variables during dropwise condensation.
3. The major portion of the heat transferred during dropwise condensation is through very small drops that are a micron or less in diameter.
4. Drops larger than a few microns in diameter act only as condensate reservoirs and do not contribute to the heat transfer.
5. Drop nucleation occurs only in areas activated by the coalescence of drops and by drop roll-off.
6. Dropwise condensation is not significantly effected by condensate thermal conductivity.
7. Dropwise condensation is not significantly effected by condensate viscosity. Capillary forces assumes the role in dropwise condensation that viscosity plays in filmwise condensation.
8. Roll-off drops move very rapidly down the condenser surface. After moving about one foot a trailing tail on the drop breaks off and stops in the roll-off track.

9. The growth rate of the drop field is a strong function of the surface temperature of the condenser.

10. The nucleation time of a drop is a strong function of the condenser surface temperature.

11. Teflon provides an excellent surface for the study of dropwise condensation.

12. The promoting property of teflon films are not effected by indefinate exposure to a 212°F steam environment. Teflon coatings were tested for 3080 hrs. without noticable deterioration.

13. Drops can only nucleate if their radius exceeds a certain critical value. At a $(T_{sv}-T_s)$ of 0.3°F the critical radius is about 1 micron, while at a $(T_{sv}-T_s)$ of 180°F, the critical radius declines to about 2.2×10^{-4} microns.

14. On a normal condenser surface capable of promoting dropwise condensation there are three types of nucleation sites. Random nucleation with respect to both location and time was analyzed and shown to produce as many as 10^{10} sites per second per square inch. Preferred wetted and non-wetted sites were observed to number about 10^{6} per square inch. The number of preferred sites is a strong function of the condition of a particular condenser surface. Preferred sites have a strong

influence on the drop growth pattern on the condenser surface.

15. The following mechanism is proposed for dropwise condensation; drops nucleate at random and preferred condensation sites located on active bare condenser surface. Most of the heat is transferred through nucleation sized drops. Nucleation sized drops grow by capturing vapor molecules. After the first collision of the nucleation sized drops the new drop field grows primarily by coalescence. Drop coalescence and roll-off provide more active surface on which nucleation again occurs.

16. Theoretical expressions were derived for the heat flux and heat transfer coefficient. These expressions were based on the proposed mechanism of dropwise condensation, the kinetic theory of gases, and the heat transfer data obtained during this program.

10.1 RECOMMENDATIONS

1. Applied research on thin plastic films should be conducted to establish a commercially feasible scheme for promoting dropwise condensation.

2. Research should be conducted to obtain data for

organic as well as metalic vapors. This data would help establish the validity of the equations that were derived from this research. Data for other vapors would also aid in the evaluation of the importance of condensate viscosity and thermal-conductivity.

11.0 BIBLIOGRAPHY

1. Reisbig, R. L., M.S. Thesis, University of Washington, 1963.

2. Topper, L., Baer, E., J. Colloid Sci., V.10, P. 225, 1955.

3. Westwatter, J. W., Welch, J. F., International Developments In Heat Transfer, ASME, Part II, P. 302, 1961.

4. McCormick, J., Baer, E., 8th Midwestern Mechanics Conference, Case Institute of Technology, 1963.

5. Shafrin, E. G., Zisman, W. A., J. Phys. Chem., V. 64, P. 519, 1960.

6. Pierce, O. R., International Science and Technology, P. 31, Nov. 1962.

7. Nagle, W. M., Drew, T. B., Trans Am. Inst. Chem. Engr., V. 30, P. 217, 1933-1934.

8. Drew, T. B., Nagle, W. M., Smith, W. C., Trans. Am. Inst. Chem. Engrs., V. 31, P. 605, 1935.

9. Fatica, N., Katz, D. L., Chem. Eng. Prog., V. 45, P. 661, 1949.

10. Welch, J. F., Ph. D. Thesis, University of Illinois, 1960.

11. Gladstone, S., Physical Chemistry, VanNostrand Co., 1947.

12. Langmuir, Surface Chemistry, Chemical Reviews, V. 13, 1933.

13. Umur, A., Griffith, P., Trans. Am. Inst. Mech. Eng., Paper No. 64-WA/HT-3, 1964.

14. Shea, F. L., Krase, N. W., Trans. Am. Inst. Chem. Engrs., V. 36, P. 463, 1940.

15. Hampson, H., Ozisik, N., Inst. of Mech. Engrs., Proceedings B, P. 282, 1952-1953.

16. Nagle, W. M., V. S. Patent 1,995,361, 1935.

17. Russell, H. W., U. S. Patent 2,248.909, 1941.

18. Hunter, J. B., U. S. Patent 2,469,729, 1949.

19. Vaaler, L. E., U. S. Patent 2,919,115, 1958.

20. Jakob, M., Mech. Engineering, V. 58, P. 729, 1936.

21. Baer, E., McKelvey, A.C.S. Delaware Science Symposium, University of Delaware, 1958.

22. Davies, J. T., Rideal, E. K., Interfacial Phenomenon, Academic Press, 1961.

23. Alty, T., Nicoll, F. H., Canadian J. Research, V. 4, P. 547, 1931.

24. Depew, C. A., Reisbig, R. L., I & EC Process Design and Development, V. 3, P. 365, 1964.

25. Jakob, M., Heat Transfer, V. 1, John Wiley and Sons, Inc., 1958.

26. Krieth, F., Principles of Heat Transfer, International Textbook Co., 1965.

27. Sugawara, S., Michiyoshi, Proceedings of The Second Japanese Natl. Congr. Appl. Mech., Part III, P. 289, 1952.

28. Grober, H., Erk, S., Grigull, J., Fundamentals of Heat Transfer, McGraw Hill Book Co., P. 327, 1961.

29. Emmons, H., Trans. AI. Ch. Eng., V. 35, P. 109, 1939.

30. Schmidt. E., Schurig, W., Sellschopp, W., Tech. Mech. U. Thermodynam., V. 1, P. 53, 1930.

31. Nusselt, W., Z. VDI, V. 60, P. 541, 1916.

32. Hill, P. G., Witting, H., Demetri, E. P., Am. Soc. Mech. Eng. J. of Heat Transfer, V. 85, No. 4, P. 303, 1963.

33. McCormick, J. D., Baer, E., J. of Colloid Science, V. 18, P. 208, 1963.

34. Tamman, G., Boeheme, W., Ann. Physik, V. 22, P. 77, 1935.

35. Fitzpatric, J. P., Baum, S., McAdams, W. H., Trans, AI. Ch. Eng., V. 35, 1939.

36. Bureau of Naval Weapons, "Process of Applying Thin Films of Polytetrafluoroethylene Resins On Aluminum Alloy Surfaces", NAVWEPS Ordnance Data 23684, Department of The Navy, Washington 25, D. C., 1961.

37. Sears, The Kinetic Theory of Gases and Statistical Mechanics, Addison Wesley Co., 1959.

38. Lee, J. F., Sears, F. W., Thermodynamics, Addison Wesley Co., 1959.

39. Hamson, H., Engineering, V. 172, No. 4464, P. 221, 1951

40. Nagle, W. N., Bays, G. S., Blenderman, L. M., Drew, T. M., Trans. AI. Ch. E, V. 31, 1934.

APPENDIX I Heat Transfer and Photographic Data

Nomenclature

Symbol		Unit
T_{st}	steam temperature in steam chamber.....	°F
T_1	temperature at the bottom and one inch behind the condenser surface.....	°F
T_2	temperature at the bottom and one inch behind the condenser surface.....	°F
T_3	temperature behind teflon at the bottom of the condenser.....	°F
T_4	temperature behind teflon at the bottom of the condenser.....	°F
T_5	temperature at the top and one inch behind the condenser surface.....	°F
T_6	temperature at the top and one inch behind the condenser surface.....	°F
T_7	temperature behind the teflon at the top of the condenser surface.....	°F
T_8	temperature behind the teflon at the top of the condenser surface.....	°F
T_{c1}	average of T_3, T_4, T_7, T_8.....	°F
T_{c2}	average of T_1, T_2, T_5, T_6.....	°F
Q_1	heat flux using $(T_{c1}-T_{c2})$.....	$\frac{BTU}{Hrft^2}$
$\dot{C}$	measured condensate rate.....	$\frac{ml}{min.}$
Q_2	heat flux using $\dot{C}$.....	$\frac{BTU}{Hrft^2}$
$Q_{av} = 0.75\ Q_2 + 0.25\ Q_1$	.....	$\frac{BTU}{Hrft^2}$
P_c	total steam pressure in test chamber...	In. of Hg
T_{sv}	saturated steam temp. at P_c.....	°F

T_s	computed surface temp. of the teflon..	°F
$\bar{h}$	computed overall heat transfer coefficient.....	$\frac{BTU}{Hrft^2°F}$
m	number of diameters of magnification	
F.S.	film speed, pictures per second	
EXP.	film exposure rating**	
FOC.	film focus rating**	
L	distance measured from the upper edge of the condenser surface.	

** E-excellent, G-good, F-fair, P-poor

HEAT TRANSFER DATA: DROPWISE CONDENSATION OF WATER VAPOR ON A 4" X 12" TEFLON COATED COPPER CYLINDER.

RUN NO.	1	2	3	4	5	6
T_{st}	214.3	214.6	215.0	214.8	214.8	215.1
T_1	197.8	196.4	197.0	195.8	200.5	164.1
T_2	196.9	195.9	195.4	194.3	200.0	164.0
T_3	203.5	201.3	201.0	199.4	203.6	181.9
T_4	206.6	204.0	203.3	201.7	205.6	182.8
T_5	197.2	194.2	194.3	193.3	198.8	165.7
T_6	196.2	193.1	193.1	192.1	196.2	165.3
T_7	198.5	199.0	199.4	199.0	201.3	180.5
T_8	203.8	199.7	199.7	199.0	201.3	182.1
T_{c1}	203.1	201.1	200.9	199.8	203.0	181.8
T_{c2}	197.5	194.9	195.0	193.9	198.9	165.0
$T_{c1}-T_{c2}$	5.6	6.2	5.9	5.9	5.1	16.8
Q_1	10,300	11,800	11,200	11,200	9,700	31,900
$\dot{c}$	88.1	102.0	101.0	100.0	88.0	238.0
Q_2	11,000	12,800	12,700	12,500	11,000	29,700
$Q_{av.}$	10,800	12,500	12,300	12,200	10,700	30,300
P_c	31.38	31.38	31.08	30.38	31.38	31.69
T_{sv}	214.4	214.4	213.9	212.8	214.4	214.9
T_s	213.9	213.6	213.2	212.0	213.7	212.1
$T_{sv}-T_s$	0.5	0.8	0.7	0.8	0.7	2.8
$\bar{h}$	21,600	15,600	17,600	15,250	15,300	10,800

HEAT TRANSFER DATA: DROPWISE CONDENSATION OF WATER VAPOR ON A 4" X 12" TEFLON COATED COPPER CYLINDER.

RUN NO.	7	8	9	10	11	12
T_{st}	215.0	214.5	215.1	215.8	215.0	214.6
T_1	169.0	180.9	188.0	188.7	189.0	190.0
T_2	169.0	180.5	189.0	188.0	189.3	190.6
T_3	182.0	189.1	195.4	195.4	196.1	199.0
T_4	182.6	192.4	196.8	197.0	196.8	201.0
T_5	175.9	180.0	188.0	189.0	189.0	193.2
T_6	174.0	180.3	187.0	187.5	189.5	192.0
T_7	185.6	191.1	194.4	195.5	196.8	197.2
T_8	186.4	192.1	196.8	196.0	196.6	198.0
T_{c1}	184.2	191.2	195.9	196.0	196.6	198.8
T_{c2}	173.1	180.4	188.0	188.3	189.2	191.5
$T_{c1}-T_{c2}$	12.3	9.8	7.9	7.7	7.4	7.3
Q_1	23,500	18,700	15,000	14,700	14,100	13,900
$\dot{c}$	200.0	160.0	123.0	125.5	119.0	103.5
Q_2	25,000	20,100	15,400	15,700	14,900	13,000
$Q_{av.}$	24,700	19,800	15,300	15,500	14,700	13,200
P_c	29.93	30.23	30.23	30.22	30.22	30.22
T_{sv}	212.0	212.5	212.5	212.5	212.5	212.5
T_s	208.9	211.0	211.2	211.5	211.3	212.0
$T_{sv}-T_s$	3.1	1.5	1.3	1.0	1.2	0.5
$\bar{h}$	8,000	13,200	11,750	15,500	12,250	26,400

HEAT TRANSFER DATA: DROPWISE CONDENSATION OF WATER VAPOR ON A 4" X 12" TEFLON COATED COPPER CYLINDER.

RUN NO.	13	14	15	16	17	18
T_{st}	216.0	215.1	215.0	215.3	215.2	215.2
T_1	190.0	191.8	171.8	177.8	177.8	155.2
T_2	190.8	191.6	169.0	175.6	174.4	152.6
T_3	198.5	199.3		187.0	185.0	
T_4	199.4	201.3	185.0	185.0	190.4	172.0
T_5	193.8	194.5	174.5	178.2	179.4	163.0
T_6	192.0	193.2	172.4	176.3	177.6	160.0
T_7	197.4	198.2	184.5	187.6	188.5	177.0
T_8	197.9	198.6	186.5	188.4	190.0	179.0
T_{c1}	198.3	199.4	185.3	187.0	187.7	176.0
T_{c2}	191.4	192.8	171.9	177.0	177.3	157.7
$T_{c1}-T_{c2}$	6.9	6.6	13.4	10.0	10.4	18.3
Q_1	13,100	12,600	25,400	19,000	19,800	34,600
$\dot{C}$	105.5	100.0	196.0	192.0	183.0	259.0
Q_2	13,200	12,500	24,500	24,000	22,800	32,400
$Q_{av.}$	13,200	12,500	24,800	22,800	22,000	33,000
P_c	30.22	30.22	30.31	30.31	30.31	30.25
T_{sv}	212.5	212.5	212.6	212.6	212.6	212.5
T_s	211.5	211.9	210.1	209.8	209.7	209.0
$T_{sv}-T_s$	1.0	0.6	2.5	2.8	2.9	3.5
$\bar{h}$	13,200	20,900	9,910	8,150	7,600	9,450

HEAT TRANSFER DATA: DROPWISE CONDENSATION OF WATER VAPOR ON A 4" X 12" TEFLON COATED COPPER CYLINDER.

RUN NO.	19	20	21	22	23	24
T_{st}	215.0	215.4	216.0	215.3	216.1	213.2
T_1	157.4	170.7	149.8	167.8	165.0	175.5
T_2	155.0	168.4	144.8	165.0	162.1	176.5
T_3			164.0	182.0	180.5	187.5
T_4	173.6	184.8	171.1	183.7	182.6	187.8
T_5	164.0	170.9	156.0	170.1	167.7	181.0
T_6	161.8	171.0	153.0	167.2	164.8	179.0
T_7	178.0	184.0	172.2	182.2	180.9	190.0
T_8	179.0	185.8	174.6	184.0	182.7	190.5
T_{c1}	177.2	184.8	170.5	183.0	181.7	189.0
T_{c2}	159.6	170.3	150.9	167.5	164.9	178.0
$T_{c1}-T_{c2}$	17.6	12.5	21.7	15.5	16.8	11.0
Q_1	33,400	23,800	41,200	29,400	31,900	21,000
$\dot{C}$	253.0	203.0	330.0	224.0	254.0	168.0
Q_2	31,600	25,400	41,200	28,000	31,800	21,000
$Q_{av.}$	32,100	25,000	41,200	28,400	31,800	21,000
P_c	30.25	30.25	32.40	31.18	32.4	30.23
T_{sv}	212.5	212.5	216.0	214.1	216.0	212.5
T_s	209.3	209.8	211.7	211.4	213.5	210.0
$T_{sv}-T_s$	3.2	2.7	4.2	2.7	2.5	2.5
$\bar{h}$	10,000	9,300	9,800	10,500	12,700	8,400

HEAT TRANSFER DATA: DROPWISE CONDENSATION OF WATER VAPOR ON A 4" X 12" TEFLON COATED COPPER CYLINDER.

RUN NO.	25	26	27	28	29	30
T_{st}	214.4	215.0	216.7	217.8	212.5	215.5
T_1	181.0	191.0	190.5	197.0	192.6	149.1
T_2	179.0	189.4	190.5	195.9	193.0	140.9
T_3	190.3	198.0	198.1	201.8		
T_4	193.7	200.8	201.3	204.5	204.2	170.1
T_5	180.3	188.4	189.2	194.1	193.6	154.0
T_6	178.8	186.6	188.0	190.8	192.4	151.0
T_7	188.4	195.0	195.6	199.4	198.8	172.1
T_8	190.0	195.7	196.2	199.8	199.3	174.1
T_{c1}	190.6	197.3	197.8	201.4	200.1	172.1
T_{c2}	179.8	188.9	189.6	194.5	192.9	153.1
$T_{c1}-T_{c2}$	10.8	8.4	8.2	6.9	7.2	19.0
Q_1	20,500	16,000	15,600	13,100	13,500	36,200
$\dot{C}$	167.0	128.0	130.0	110.5	100.0	300.0
Q_2	20,900	16,000	16,300	13,800	12,500	37,500
$Q_{av.}$	20,800	16,000	16,100	13,600	12,700	37,200
P_c	30.86	31.66	31.66	32.26	31.06	30.86
T_{sv}	213.6	214.9	214.9	215.8	213.9	213.6
T_s	211.4	213.3	213.9	215.0	212.8	209.3
$T_{sv}-T_s$	2.2	1.6	1.0	0.8	1.1	4.3
$\bar{h}$	9,460	10,000	16,100	17,000	12,500	8,650

HEAT TRANSFER DATA: DROPWISE CONDENSATION OF WATER VAPOR ON A 4" X 12" TEFLON COATED COPPER CYLINDER.

RUN NO.	31	32	33	34	35	36
T_{st}	215.0	215.0	215.1	215.3	215.2	215.1
T_1	167.0	147.3	135.2	154.2	131.6	125.8
T_2	164.1	141.4	124.3	150.2		
T_3	182.1	163.0	146.0	176.0		
T_4	183.0	174.5	166.0	178.7	160.5	155.5
T_5	167.9	151.2	142.5	160.5	145.0	140.1
T_6	165.3	148.3	139.7	157.0	143.5	138.5
T_7	180.5	169.4	165.0	178.2	167.0	162.5
T_8	182.1	172.0	167.5	180.4	168.1	164.3
T_{c1}	181.4	169.7	161.1	178.3	165.2	160.8
T_{c2}	166.1	147.1	135.4	155.5	140.0	134.8
$T_{c1}-T_{c2}$	16.6	22.6	25.7	22.7	25.2	26.0
Q_1	31,500	42,900	48,600	43,100	47,900	49,400
$\dot{c}$	239.0	330.0	367.0	271.0	323.0	369.0
Q_2	29,900	41,300	45,900	33,800	40,400	46,000
$Q_{av.}$	30,300	41,700	46,600	34,100	42,300	46,900
P_c	31.69	31.69	31.34	31.69	31.02	31.02
T_{sv}	214.9	214.9	214.3	214.9	213.8	213.8
T_s	211.7	211.4	207.7	212.4	207.5	207.7
$T_{sv}-T_s$	3.2	3.5	6.6	2.5	6.3	6.1
$\bar{h}$	9,450	11,900	7,100	13,600	6,710	7,700

HEAT TRANSFER DATA: DROPWISE CONDENSATION OF WATER VAPOR ON A 4" X 12" TEFLON COATED COPPER CYLINDER.

RUN NO.	37	38	39	40	41	42
T_{st}	214.8	214.9	215.0	215.0	215.3	215.2
T_1	140.0	142.8	135.8	144.4	118.0	142.2
T_2	141.2	135.4	128.3			
T_3		154.4				
T_4	161.8	167.0	161.3	170.1	156.0	168.5
T_5	147.3	150.4	144.2	151.8	133.1	151.0
T_6	144.9	147.5	141.4	149.8	131.6	148.5
T_7	163.0	168.5	163.3	170.5	154.8	169.5
T_8	166.4	171.1	166.3	172.5	156.0	172.0
T_{c1}	163.7	165.2	163.6	171.0	155.6	170.0
T_{c2}	143.4	144.0	137.4	145.5	127.6	147.2
$T_{c1}-T_{c2}$	20.3	25.0	26.2	22.4	28.0	22.8
Q_1	38,600	47,500	49,600	42,400	53,200	43,400
$\dot{c}$	347.0	347.0	357.0	305.0	382.0	307.0
Q_2	43,400	43,400	45,600	38,200	48,000	38,400
$Q_{av.}$	42,200	44,400	46,600	39,200	49,300	39,600
P_c	30.60	31.60	31.60	31.13	30.10	31.30
T_{sv}	213.1	214.8	214.8	214.0	212.3	214.3
T_s	205.9	209.6	210.2	210.2	204.9	209.6
$T_{sv}-T_s$	7.2	5.2	4.6	3.8	7.4	4.7
$\bar{h}$	5,860	8,500	10,000	10,300	6,650	8,450

HEAT TRANSFER DATA: DROPWISE CONDENSATION OF WATER VAPOR ON A 4" X 12" TEFLON COATED COPPER CYLINDER.

RUN NO.	43	44	45	46	47	48
T_{st}	215.0	215.0	214.5	216.0	215.0	215.0
T_1	155.8	179.4	185.4	167.0	164.1	147.3
T_2	151.0	177.0	183.9	164.1	161.3	141.4
T_3		189.5	193.8	182.1	181.9	163.0
T_4	176.9	192.7	197.0	184.0	183.6	170.5
T_5	161.0	179.0	183.6	167.9	165.7	151.2
T_6	158.5	177.0	182.1	165.3	163.3	148.3
T_7	175.8	188.1	191.5	180.5	180.0	169.4
T_8	177.7	189.6	193.0	180.1	181.1	172.0
T_{c1}	176.8	190.0	193.8	181.7	181.7	168.7
T_{c2}	156.6	178.1	183.8	166.1	163.6	147.1
$T_{c1}-T_{c2}$	20.2	11.9	10.0	15.5	18.1	21.6
Q_1	38,400	22,600	19,000	29,400	34,200	41,000
$\dot{c}$	257.0	177.0	150.0	239.0	238.0	330.0
Q_2	32,200	22,200	18,750	29,900	29,700	41,300
$Q_{av.}$	33,800	22,300	18,800	29,800	30,100	41,200
P_c	30.90	31.30	31.46	31.34	31.35	31.34
T_{sv}	213.7	214.3	214.5	214.3	214.4	214.3
T_s	210.6	212.3	212.6	211.5	211.8	209.9
$T_{sv}-T_s$	3.1	2.0	1.9	2.8	2.6	4.4
$\bar{h}$	10,900	11,100	9,900	10,650	11,150	9,380

MOTION PICTURE AND HEAT TRANSFER DATA: DROPWISE CONDENSATION OF WATER VAPOR ON A 4" X 12" TEFLON COATED COPPER CYLINDER.

RUN NO.	M-1	M-2	M-3	M-4	M-5	M-6
T_{st}	214.0	214.0	214.0	212.5	212.5	212.6
T_3	194.3	194.3	194.3	186.4	186.4	186.4
T_4	196.0	196.0	196.0	187.4	187.4	187.4
T_7	191.5	191.5	191.5	185.4	185.4	185.4
T_8	193.0	193.0	193.0	186.2	186.2	186.2
T_{c1}	193.7	193.7	193.7	186.0	186.0	186.0
$\dot{C}$	150	150	150	192	192	192
Q_2	18,750	18,750	18,750	24,000	24,000	24,000
P_c	31.50	31.50	31.50	30.22	30.22	30.22
T_{sv}	214.6	214.6	214.6	212.5	212.5	212.5
T_s	212.5	212.5	212.5	210.0	210.0	210.0
$T_{sv}-T_s$	2.1	2.1	2.1	2.5	2.5	2.5
$\bar{h}$	8,900	8,900	8,900	9,600	9,600	9,600
m	18.5	10.0	4.6	10.0	4.6	4.6
F.S.	1,700	1,700	1,700	1,000	1,560	1,560
EXP.	P	P	G	F	E	E
FOC.	F	G	G	F	G	E
L	5.0	5.0	5.0	5.0	5.0	0.0

MOTION PICTURE AND HEAT TRANSFER DATA: DROPWISE CONDENSATION OF WATER VAPOR ON A 4" X 12" TEFLON COATED COPPER CYLINDER.

RUN NO.	M-7	M-8	M-9	M-10	M-11	M-12
T_{st}	212.5	212.5	212.5	212.5	212.3	212.3
T_3	186.4	186.4	186.4	186.4	198.5	198.5
T_4	187.4	187.4	187.4	187.4	198.5	198.5
T_7	185.4	185.4	185.4	185.4	196.4	196.4
T_8	186.2	186.2	186.2	186.2	196.8	196.8
T_{cl}	186.0	186.0	186.0	186.0	197.5	197.5
$\dot{C}$	192	192	192	192	109	109
Q_2	24,000	24,000	24,000	24,000	13,900	13,900
P_c	30.22	30.22	30.22	30.22	30.18	30.18
T_{sv}	212.5	212.5	212.5	212.5	212.4	212.4
T_s	210.0	210.0	210.0	210.0	211.4	211.4
$T_{sv}-T_s$	2.5	2.5	2.5	2.5	1.0	1.0
$\bar{h}$	9,600	9,600	9,600	9,600	13,900	13,900
m	10.0	4.6	10.0	0.124	0.124	0.124
F.S.	1,560	1,560	9,60	2,400	2,500	2,500
EXP.	F	G	F	E	G	F
FOC.	F	G	G	E	G	G
LOC.	0.0	9.0	9.0	9.0	11.8	6.0
V_d				30.0	55.0	29.5

MOTION PICTURE AND HEAT TRANSFER DATA: DROPWISE CONDENSATION OF WATER VAPOR ON A 4" X 12" TEFLON COATED COPPER CYLINDER.

RUN NO.	M-13	M-14	M-15	M-16	M-17	M-18
T_{st}	213.3	213.3	213.3	213.3	213.0	213.0
T_3	198.5	198,5	198.5	198.5	186.4	173.7
T_4	198.5	198.5	198.5	198.5	187.4	177.2
T_7	196.4	196.4	196.4	196.4	185.8	174.1
T_8	196.8	196.8	196.8	196.8	186.2	177.0
T_{c1}	197.5	197.8	197.8	197.8	186.5	175.0
$\dot{c}$	109	109	109	109	192	276
Q_2	13,900	13,900	13,900	13,900	24,000	34,500
P_c	30.18	30.18	30.18	30.18	30.45	30.45
T_{sv}	212.4	212.4	212.4	212.4	212.9	212.9
T_s	211.4	211.4	211.4	211.4	210.5	209.5
$T_{sv}-T_s$	1.0	1.0	1.0	1.0	2.4	3.4
$\bar{h}$	13,900	13,900	13,900	13,900	10,000	10,100
m	0.124	4.6	4.6	4.6	0.124	4.6
F.S.	2,500	720	1,200	1,200	2,400	1,200
EXP.	F	E	P	E	F	E
FOC.	G	E	P	G	G	G
LOC.	0.0	0.0	5.0	9.0	0.0	9.0
V_d	8.0				12.1	

MOTION PICTURE AND HEAT TRANSFER DATA: DROPWISE CONDENSATION OF WATER VAPOR ON A 4" X 12" TEFLON COATED COPPER CYLINDER.

RUN NO.	M-19	M-20
T_{st}	213.0	213.0
T_3	173.7	173.7
T_4	177.2	177.2
T_7	174.1	174.1
T_8	177.0	177.0
T_{c1}	175.0	175.0
$\dot{C}$	276	276
Q_2	34,500	34,500
P_c	30.45	30.45
T_{sv}	212.9	212.9
T_s	209.5	209.5
$T_{sv}-T_s$	3.4	3.4
$\bar{h}$	10,100	10,100
m	4.6	4.6
F.S.	1,200	1,200
EXP.	E	G
FOC.	E	E
LOC.	5.0	0.0

APPENDIX II Error Analysis of The Data.

An estimate of the degree of uncertainty in the experimental measurements for the heat transfer coefficient is presented below. The word "uncertainty" is used to signify the outer limits of confidence within which a measurements lies.

The heat transfer coefficient was calculated from basic data using the following equation,

$$\bar{h} = \frac{Q}{(T_{sv}-T_s)} \qquad (1)$$

Where: Q= heat flux, BTU/Hr/ft^2

The condenser surface temperature was determined from the following equation,

$$T_s = T_{cl} + \frac{t}{k} Q \qquad (2)$$

Where: T_{cl} = average measured temperature behind the teflon coating.

t = thickness of the teflon.

k = thermal conductivity of the teflon.

For a given data point $\bar{h}$ is a function of the following variables,

$$\bar{h} = f(Q, T_{sv}, T_s) \qquad (3)$$

Thus, the uncertainty of $\bar{h}$ is given by,

$$\delta \bar{h} = \frac{\partial f}{\partial Q} \delta Q + \frac{\partial f}{\partial T_{sv}} \delta T_{sv} + \frac{\partial f}{\partial T_s} \delta T_s \qquad (4)$$

The derivatives of f in equation (4) can be evaluated from equation (1) giving,

$$\delta \bar{h} \leq \left| \frac{1}{T_{sv}-T_s} \delta Q \right| + \left| \frac{Q}{(T_{sv}-T_s)^2} \delta T_{sv} \right| + \left| \frac{Q}{(T_{sv}-T_s)^2} \delta T_s \right| \qquad (5)$$

The uncertainty of the experimental data for Q, and T_{sv} can be stated, however, the uncertainty of the surface temperature T_s must be evaluated from equation (2).

$$T_s = F(T_{cl}, Q, t, k) \qquad (6)$$

So

$$\delta T_s = \frac{\partial F}{\partial T_{cl}} \delta T_{cl} + \frac{\partial F}{\partial Q} \delta Q + \frac{\partial F}{\partial t} \delta t + \frac{\partial F}{\partial k} \delta k \qquad (7)$$

By using equation (2) to evaluate the derivatives in equation (7), one gets,

$$\delta T_s \leq \left| \delta T_{cl} \right| + \left| \frac{t}{k} \delta Q \right| + \left| \frac{Q}{k} \delta t \right| + \left| \frac{tQ}{k^2} \delta k \right| \qquad (8)$$

Since the maximum uncertainty is being evaluated, all derivatives in equations (4) and (7) were assigned positive values.

The uncertainty of T_s is shown to be a function of the teflon thickness t. Any error in the measurement of t will be reflected in the data as a fixed error.

The teflon thickness was determined by measuring the outside diameter of the copper test cylinder both before and after it was coated. The measurement was made with a micrometer that could be read to the nearest 0.0001 inch. The teflon thickness used in the calculations (0.0017 inch) is an average value determined by a large number of measurements. The maximum variation in the cylinder diameter was about 0.002 inches before it was coated. The diameter variation of the coated cylinder was also about 0.002 inches. After the experiments were completed, the teflon film was stripped from the areas directly over the thermocouples. These pieces were measured with a micrometer and their thicknesses were found to be 0.0017 inch $\pm$ 0.00008 inch. Strips of teflon film were also removed from other portions of the condenser surface and were found to measure 0.0017 inch $\pm$0.00008 inch. The standard deviation of the thickness measurements was 0.00008 inches, and will be assumed to be the uncertainty in the teflon thickness.

The copper-constantan thermocouples used to determine T_{c1} were all calibrated at the ice point and at the steam point. Each thermocouple was accurate to $\pm$0.1°F at these temperatures. The potentiometer used to record the temperatures was accurate to less than 0.05°F at the steam point.

The variation of the condensate rate measurement used to measure Q was smallest when the heat flux was small since the time required to collect 1000 ml of condensate was longest. For the higher condensate rates (300 ml/min.) there may have been a $\pm$ 1 sec. error in determining the time. This would give an uncertainty of about 2-3 ml/min. in the condensate rate.

The saturated vapor temperature was derived from the steam chamber pressure which could be read to $\pm$ 0.1 inch of Hg.

The uncertainty of the various experimental parameters can be deduced from the above discussion as follows.

$$\delta Q = 300 \text{ BTU/hr/ft}^2$$

$$\delta T_{cl} = 0.2^\circ F$$

$$\delta T_{sv} = 0.2^\circ F$$

$$\delta t = 0.00008 \text{ inch}$$

$$\delta k = 0.001 \text{ BTU/Hr/ft/F}$$

The uncertainty of T_s and $\bar{h}$, using the above numbers and equation (5), is presented below at two values of $(T_{sv}-T_s)$.

$(T_{sv}-T_s)$	δT_s	$\delta \bar{h}$
4.2	2.4	6,160 BTU/hr/ft^2/°F
7.4	2.7	2,620 BTU/hr/ft^2/°F

The abcve uncertainty values can be compared with the data which are presented in figure 3.2 on page 26. The data from this program are shown to be within the predicted uncertainty values. Note that the Nusselt equation (eqn. 7.1.1) is used as the lower boundary of the uncertainty.

The heat transfer coefficient and the condenser surface temperature may have been effected by the following factors during the experiment.

1. Temperature variation caused by the heating of the cooling water as it passed through the test section.

2. Small traces of non-condensable air in the test chamber.

3. Vapor velocity and distribution in the test chamber.

During the experiment, every attempt was made to control or eliminate the above factors. It is assumed that these phenomena did not significantly effect the data.

APPENDIX III Sample Calculations

The following calculations are typical of the method used to reduce the data. The example represents the data from run number 1 of Appendix I. Consider the following sketch of the condenser surface cross section.

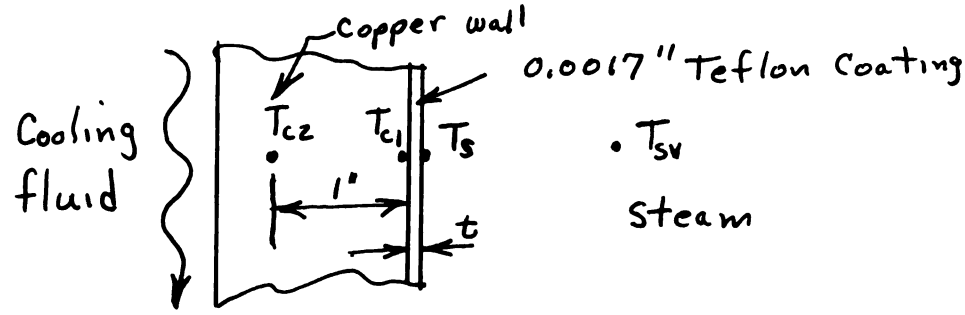

The heat conducted across the teflon is,

$$Q/A = \frac{k}{t} \quad (T_s - T_{c1}) \tag{1}$$

Thus, the surface temperature is given by

$$T_s = Q/A \cdot \frac{t}{k} + T_{c1} \tag{2}$$

Using the properties of teflon egn. 2 becomes,

$$T_s = \frac{Q/A}{1000} + T_{c1} \tag{3}$$

The heat conducted through the copper is given by

$$Q_1 = Q/A = \frac{k}{r_1 \ln\left(\frac{r_1}{r_2}\right)} \quad (T_{c1} - T_{c2}) \tag{4}$$

or,

$$Q_1 = 1900\ (T_{c1}-T_{c2}) \tag{5}$$

From run number 1 of the heat transfer data,

$$T_{c1} = 203.1\ ^\circ F$$

$$T_{c2} = 197.5\ ^\circ F$$

$$(T_{c1}-T_{c2}) = 5.6\ ^\circ F$$

Using equation 5 gives,

$$Q_1 = 10{,}300\ \ BTU/hrft^2 \tag{6}$$

The condensate data is given as,

$$\dot{C} = 88.1\ ml/min.$$

$$Q_2 = 125\ \dot{C} = 11{,}000\ BTU/hrft^2 \tag{7}$$

The data was weighed in favor of the condensate rate data as follows,

$$Q_{av.} = 0.75Q_2 + 0.25Q_1 = 10{,}800\ BTU/hrft^2 \tag{8}$$

The saturated vapor temperature was taken from, "Thermodynamic Properties of Steam", by Keenan and Keyes, at the measured steam chamber pressure P_c. Thus for run No. 1,

$$T_{sv} = 214.4\ ^\circ F \tag{9}$$

The surface temperature of the teflon film is calculated from equation 3 as,

$$T_s = \frac{Q_{av}}{1000} + T_{cl} = 213.9\ ^\circ F \qquad (10)$$

The average heat transfer coefficient is,

$$\bar{h} = \left(\frac{Q_{av}}{T_{sv} - T_s}\right) \qquad (11)$$

$$(T_{sv} - T_s) = 0.5\ ^\circ F$$

Thus;

$$\bar{h} = \frac{10{,}800}{0.5} = 21{,}600 \quad BTU/hrft^2\ ^\circ F$$

APPENDIX IV Boiler Water Analysis

Table I Chemical analysis of a raw 16oz. sample of water used by Michigan State University Power Plants.

Total hardness ($CaCO_3$).....	303
Calcium (Ca).....	81
Magnesium (Mg).....	24
Chloride (Cl).....	2
Sulfate (So_4).....	17
Nitrate (No_3).....	0
Silica (Sl O_2).....	16.7
Iron and Alumina.....	0.2
Bicarbonate (HCo_3).....	375
Sodium (Na).....	12
Total disolved solids.....	337
pH.....	7.8

APPENDIX IV Boiler Water Analysis (continued)

Table II Chemical analysis of four samples of water used in the boilers.

Sample

#1 8 oz. make-up water sample

#2 8 oz. feed water sample

#3 boiler sample

#4 boiler sample

	#1	#2	#3	#4
Hardness($CaCO_3$)			0	0
Sodium Hydroxide(NaOH)			2.0	0.1
Sodium Carbonate($NaCO_3$)			2.0	1.9
Sodium Chloride(NaCl)			0	0
Sodium Sulfate(Na_2SO_4)			0.5	0.8
Sodium Nitrate($NaNO_3$)			0	0
Sodium Phosphate(PO_4)			16	19
Silica(SiO_2)	0.16	0.17	11	5.0
Total dissolved solids	3.1	1.8	111	75
pH value	6.4	8.5	11.1	10.4
CO_2	1.25	0		
NH_3	0.03	0.18		

All the above numbers except the pH values have the units of parts per million.

MICHIGAN STATE UNIV. LIBRARIES
31293010748956